https://doi.org/10.5194/egusphere-2025-1573
Preprint. Discussion started: 13 May 2025

Unprecedented radioactive pollution in Spitsbergen air - first data as of 21st century

Anna Cwanek[1*], Agnieszka Burakowska[2], Ewa Nalichowska[1], Magdalena Długosz-Lisiecka[3], Marek Kubicki[4], Tomasz Wawrzyniak[4], Edyta Łokas[1], Michał Gryziński[2], Kamil Brudecki[1]

[1]Institute of Nuclear Physics, Polish Academy of Sciences, 31-342 Kraków, Poland
[2]National Centre for Nuclear Research, 05-400 Otwock-Świerk, Poland
[3]Lodz University of Technology, Institute of Applied Radiation Chemistry, 90-924 Łódz, Poland
[4]Institute of Geophysics, Polish Academy of Science, 01-452 Warszawa, Poland

Correspondence to: Anna Cwanek (anna.cwanek@ifj.edu.pl)

Abstract. The present study concerned the Arctic troposphere, providing an experimental database on nuclear aerosols that has improved considerably since 1999. The activity concentrations of ^{238}Pu, $^{239+240}$Pu and ^{241}Am were determined in the surface air of Hornsund, Spitsbergen, during 2007−2021. A multivariate approach was employed, incorporating meteorological data, ^{7}Be, ^{137}Cs, ^{210}Pb records and isotopic ratios, to explain the transuranium dynamics of changes and provenance. ^{238}Pu and $^{239+240}$Pu levels were comparable to recent observations from various locations. The highest activity concentrations of 6.61 nBq/m^3 for ^{238}Pu and 15.51 nBq/m^3 for $^{239+240}$Pu identified in 2015 could be due to fly ash particles following wildfires in proximity to the Chernobyl zone. During the remaining period, $^{239+240}$Pu correlated with seasonal processes, such as local resuspension and horizontal tropospheric transport of haze layers from remote areas. Similar mechanisms likely regulated a portion of ^{238}Pu. However, further evaluation revealed a frequent occurrence of ^{238}Pu enrichment regarding known nuclear events. ^{241}Am exhibited particularly high values, with a maximum of 354 nBq/m^3 detected in 2019. Additionally, unexpected single incidents of ^{237}Np were encountered in 2013, 2014 and 2018. Unusual elevated levels of ^{241}Am, ^{238}Pu and ^{237}Np were not associated with environmental processes; therefore, the possibility of recent anthropogenic emissions should be considered. Trajectory simulations performed in 2019 showed prominent transport pathways to the Hornsund from northern Eurasia.

1 Introduction

Advances in nuclear science during the 20th century have led to the systematic production of a novel form of environmental contamination on a global scale. Introduced radionuclides, commonly classified as artificial, technogenic, man-made or anthropogenic, were previously non-existent or present in ultra-trace quantities across the Earth system. Although the nuclear era continues today, it has undergone significant changes in terms of scope, objectives and main directions over time. The initial focus on military applications has since evolved towards the development of nuclear power plants, nuclear medicine and all radioactive materials-handling industries. Undoubtedly, the ongoing revolution has brought a plethora of

https://doi.org/10.5194/egusphere-2025-1573
Preprint. Discussion started: 13 May 2025

benefits. However, the parallel identification of new radionuclide emissions and transportation over long distances from the epicentre, with the potential to increase natural background radiation levels, has raised public awareness of the necessity to monitor and control the radiological situation routinely. These measures are required not only for critical groups, objects, or areas but also to review the exposures of the population and surroundings at large. Standards of safety for radiological protection established by international or intergovernmental organisations such as the International Atomic Energy Agency (IAEA), the Commission of the European Communities (CEC), and the Organisation for Economic Co-operation and Development/Nuclear Energy Agency (OECD/NEA) are based on conceptual frameworks, as proposed by the International Commission on Radiological Protection (ICRP) (Engelbrecht and Schwaiger, 2008; ICRP, 1991, 2007). Monitoring of radioactivity levels in the air appears of particular importance, given that inhalation represents a significant exposure pathway.

The injection of anthropogenic radionuclides (^{54}Mn, ^{55}Fe, $^{89, 90}$Sr, ^{95}Zr,$^{103, 106}$Ru, ^{125}Sb, ^{131}I, $^{133, 135}$Xe, $^{134, 135, 137}$Cs, $^{141, 144}$Ce, ^{236}U, ^{237}Np, $^{238, 239, 240, 241}$Pu, ^{241}Am, $^{242, 243, 244}$Cm, etc.) into the total environment has been the consequence of a variety of specific events (UNSCEAR, 1993, 2000a), as outlined below:

(a) nuclear explosions and safety tests (> 2300):

• 543 atmospheric nuclear weapon tests (1945−1980) with legacy of global fallout (GF),

• underwater/underground nuclear weapon tests,

• sub-critical safety trials to burn or explode U and/or Pu without a fission yield,

(b) releases from nuclear reprocessing plants (NRP) and plutonium production plants (PPP), e.g. Sellafield, Cap La Hague, Mayak, Tomsk,

(c) nuclear reactor accidents in nuclear power plants (NPP), e.g. Chernobyl, Fukushima,

(d) satellite, aircraft and submarine accidents, e.g. SNAP 9A, Cosmos 954, Thule, Komsomolets K-278,

(e) effluents from nuclear installations,

(f) leaching from dumped nuclear material,

(g) U-mining and tailing,

(h) conventional explosions, including depleted uranium (DU) weapons.

Radioactive debris, once released into the atmosphere, rapidly attaches to ambient aerosol particles, being subject to the mechanisms that govern air movement. A minimum of four factors must be given consideration when investigating aerosols' forward transportation and later deposition. Firstly, the cooled debris is slowed and eventually halted within the stratosphere by the stability of the air. It is subsequently scattered by eddy diffusion into the broad layers and distributed around the globe and across a wide range of latitudes (Feely et al., 1989; UNSCEAR, 1982). When stratospheric air is carried downward—a process most common at middle latitudes and most rapid during the late winter/early spring seasons—fission products are transported into the upper layers of the troposphere (Feely et al., 1989). The mean residence time for nuclear aerosols that reach the stratosphere has been estimated to be approximately 1.5 ± 0.5 y (Hirose and Povinec, 2015). Secondly, the decreased stability of the troposphere during the warmer months results in an increased rate of vertical transport of aerosols

https://doi.org/10.5194/egusphere-2025-1573
Preprint. Discussion started: 13 May 2025

from the upper troposphere to the middle and lower troposphere and into the ground layers (Aegerter et al., 1966). A convective circulation that carries the surface air upwards and brings air from higher altitudes downwards is triggered by solar heating. The increased rate of vertical transport within the troposphere is especially pronounced during the spring/summer seasons at middle latitudes (Aegerter et al., 1966). For Arctic regions, the stability of polar atmospheric layers inhibits the vertical transport of aerosols from the upper troposphere to the surface air, even during the warmer months. The third cause, particularly in the context of high-latitude sites, pertains to the impact of seasonal variations in the transportation of tropospheric air masses from middle latitudes to high latitudes. The arrival of haze layers in the Arctic is believed to involve air pollutants emanating from middle-latitude regions of Asia, Europe, and potentially North America (Rahn, 1981). The delivery rates of haze particles to the Arctic have been attributed to a combination of annual fluctuations in the transport regime and changes in pollutant removal (Barrie et al., 1981). Such horizontal transfer phenomena are known to peak during the late winter/early spring seasons. The fourth major reason for the temporal trends of airborne radioactivity relates to the varying rate of washout of radionuclide-bearing atmospheric aerosols at sites where there are strong seasonal changes in rainfall amount and frequency (Feely et al., 1989).

It is believed that no significant quantities of artificial radionuclides remain in the stratosphere, as the majority of contaminants derived from past atmospheric emissions (primarily attributable to nuclear weapons testing) had already been descended (Hirose et al., 2003; Kierepko et al., 2016). The primary mechanism for maintaining small residual anthropogenic radioactivity above the ground level is considered to be predominantly regulated by the resuspension phenomenon (Hirose and Povinec, 2015). Atmospheric resuspension, representing a secondary source of contamination, arises from processes such as wind erosion of soil particles, sea spray effects, flying ashes from biomass burning or global desert dust events (Masson et al., 2010, 2021). Additionally, volcanic eruptions have been hypothesised to enhance the redistribution of anthropogenic radionuclides from the stratosphere to the troposphere (Alvarado et al., 2014). On the other hand, the recent worldwide releases of ^{131}I and $^{134, 137}$Cs from the Fukushima Daiichi Nuclear Power Plant (FDNPP) accident in 2011 (Koo et al., 2014; Povinec et al., 2013), along with a 2017 episode of ^{106}Ru in the air over Europe (Bossew et al., 2019), evidence that nuclear incidents may occur in the present day. Continuous measurements of activity concentrations in the atmosphere provide one of the best means of identifying and differentiating between resuspended or freshly released radioisotopes. Furthermore, the network of air monitoring stations, when used in conjunction with modelling tools, enables the radioactive plume to be traced back to the point of discharge.

The investigation of nuclear aerosols commenced in the late 1960s and early 1970s. Radioactive air sampling may be performed for one or more of the following purposes: (a) worker health protection, to ensure that worker exposures are within acceptable limits and As Low As Reasonably Achievable (ALARA), (b) environmental monitoring, to ensure that releases of radioactive aerosols into the environment are within acceptable limits and ALARA, (c) process quality assurance and control, to ensure that all procedures are functioning properly, (d) emergency preparedness and response, to provide a basis for appropriate action if an incident occurs (Hoover and Maiello, 2010). One of the most extensive and detailed records on atmospheric radioactivity in the world—the formerly Surface Air Sampling Program (SASP)—was conducted by the

https://doi.org/10.5194/egusphere-2025-1573
Preprint. Discussion started: 13 May 2025

Environmental Measurements Laboratory (EML) between 1963 and 1999 (Larsen et al., 1995), building upon the Naval Research Laboratory (NRL) idea as of 1957–1962 (U.S. Atomic Energy Commission, U.S. Energy Research and Development Administration, U.S. Department of Energy). SASP's primary objective was to determine the spatial and temporal distribution of specific natural and artificial gamma, beta and alpha emitters (^{7}Be, ^{54}Mn, ^{55}Fe, ^{89}Sr, ^{95}Zr, ^{109}Cd, ^{137}Cs, $^{141, 144}$Ce, ^{210}Pb, $^{238, 239+240}$Pu) in the ground-level air layers from monitoring stations worldwide. In addition to the radioactive debris of GF origin, the EML program has detected and characterized post-Chernobyl fallout transported across North America in 1986 (Feely et al., 1988; Larsen et al., 1989), as well as the minute quantities of fission products in Alaska after accidental releases from the Tomsk-7 nuclear complex in 1993 (Larsen 1994). The implementation of SASP was not limited solely to routine monitoring but contributed to a number of scientific observations and discoveries. Notably, the collated database enhanced the modelling of trajectories of natural and artificial aerosols within the atmosphere or revealed seasonal cycles of ^{7}Be concentrations in surface air (Feely et al., 1989) alongside the linkage between a decrease in the production rate of cosmogenic radionuclides with an increase in solar activity (Larsen, 1993). Finally, the SASP database has been introduced to the simulation of the world distributions of ^{222}Rn and ^{210}Pb using EML's three-dimensional global transport model (Lee and Feichter, 1995).

Presently, the vast majority of countries possess nationwide air-monitoring capabilities and participate in internationally coordinated network systems (e.g. CTBTO or Ro5 networks) (Baré et al., 2023; Coyne et al., 2012; Furuno et al., 2024; Steinhauser et al., 2014). Such cooperation facilitates the acquisition of data essential for assessing the radiological situation across the entire territory. This includes even remote Arctic nations (with the exception of Greenland and the Faroe Islands) and the Antarctic region (AMAP, 2015; Gorzkiewicz et al., 2022). Early detection stations for atmospheric contamination are in continuous operation, providing rapid information on selected natural (^{7}Be, ^{22}Na, ^{40}K, ^{210}Pb, etc.) and possible artificial (^{54}Mn, ^{60}Co, ^{95}Zr, $^{103, 106}$Ru, ^{125}Sb, ^{131}I, $^{133, 135}$Xe, $^{134, 137}$Cs, ^{144}Ce, ^{241}Am, etc.) radioisotopes by gamma spectrometry. Some laboratories additionally utilise alpha spectrometry or mass spectrometry to determine the presence of $^{238, 239, 240}$Pu or ^{241}Am (artificial actinides) from air filter samples. As a rule, the latter assessment is carried out in the context of a specific event and covers only a limited time interval (Alvarado et al., 2014; Chamizo et al., 2010; Masson et al., 2010). Longer-term studies are also performed; however, these are less common (Kierepko et al., 2016; Lujaniene et al., 2012; Nalichowska et al., 2023).

In certain regions, no air monitoring programs dedicated to anthropogenic actinides have been conducted since 2000. This is particularly evident for atmospheric radioactivity of the Arctic, where data on level, isotopic signature or temporal variation of $^{238, 239, 240}$Pu and ^{241}Am are lacking over the 21st century. For several reasons, research in this domain is still of particular interest and importance. The artificial actinides have attained a tracer status in investigations of atmospheric circulations or natural 'feeder' mechanisms through which previously deposited contaminants are transferred back to the air (Alvarado et al., 2014; Hirose et al., 2003; Hirose and Povinec, 2015; Masson et al., 2010). Moreover, $^{238, 239, 240}$Pu and ^{241}Am are recognised as the most radiotoxic elements that may be directly inhaled with aerosols or accumulated in plants and animals. Also noteworthy are the relatively long half-lives of these radionuclides ($^{238, 239, 240}$Pu: $T_{1/2}$ = 87.7 y, 2.41 10^{4} y, 6.56 10^{3} y,

https://doi.org/10.5194/egusphere-2025-1573
Preprint. Discussion started: 13 May 2025

respectively, ^{241}Am: $T_{1/2}$ = 432.6 y), implying that such pollution remains in the environment for a considerable duration. In the context of potential terrorist attacks involving 'dirty bombs', undeclared nuclear activity or any intentional or unintentional releases from nuclear installations, there is an imperative for the development of novel monitoring strategies (Mietelski and Povinec, 2020). Specifically, the world's national and international nuclear safety monitoring networks should incorporate routine measurements of pure beta and alpha emitters in the atmosphere.

The research project outlined in this paper aimed to address the limitations in database capabilities and to enhance the understanding of the relevant processes for artificial actinides suspended in the ground-level air layers of Hornsund, SW Spitsbergen, during the years 2007–2021. The following key objectives were specified and subsequently accomplished:

(a) determination of activity concentrations of ^{238}Pu, $^{239+240}$Pu and ^{241}Am,

(b) evaluation of mutual correlations of ^{238}Pu, $^{239+240}$Pu, ^{241}Am vs. ^{7}Be, ^{137}Cs, ^{210}Pb, suspended dust and selected meteorological factors,

(c) analysis of seasonality and long-term trends in time series of ^{238}Pu, $^{239+240}$Pu and ^{241}Am,

(d) estimation of ^{238}Pu/$^{239+240}$Pu and ^{241}Am/$^{239+240}$Pu activity ratios.

2 Materials and methods

2.1 Study area and sampling

Currently, the long-term observation of atmospheric radioactivity in the Arctic environment constitutes a central aspect of the Arctic Monitoring and Assessment Programme (AMAP) (AMAP, 2002, 2009, 2015). The geographical locations of air filter stations across the northern regions, including Iceland, the Canadian Arctic, northern Finland, Sweden and Norway with the Svalbard archipelago are illustrated in Fig. 1b. To the best of our knowledge, no coordinates are publicly available for nuclear aerosol samplers placed in the Russian Arctic (AMAP, 2009, 2015), consequently, these stations are not represented on the map.

Air monitoring of radioisotopes carried out at the Stanisław Siedlecki Polish Polar Station (77°00′ N, 15°33′ E, 10 m a.s.l.) is one of a few operating units north of the Arctic Circle (Burakowska et al., 2021) (Fig. 1d). The Polish Polar Station, situated 300 m from the shore of Isbjørnhamna Bay of the Hornsund fjord in SW Spitsbergen, Svalbard archipelago (Figs. 1a, 1c), was established during the International Geophysical Year in 1957. This northernmost permanent Polish scientific site has evolved over the years into a modern interdisciplinary scientific platform conducting research projects to better understand the functioning of the Arctic environment and the changes it undergoes (Wawrzyniak and Osuch, 2020).

A high-performance air intake system of the AZA-1000 model was launched at Hornsund in 2002 for continuous operation at low temperatures (Burakowska et al., 2021). Aerosols are collected on Petrianov filters, type FPP-15-1.5—a material composed of postchlorinated polyvinylchloride (CPVC) fibre with a high retention capacity for particles of a diameter not less than 0.3 µm. The efficiency of the FPP-15-1.5 filter for aerosols with diameters between 0.3 and 1.25 µm, at linear air velocities through the filter varying from 0.25 to 0.4 m/s, falls within the range of 96−99% (Kierepko et al., 2016). The high

https://doi.org/10.5194/egusphere-2025-1573
Preprint. Discussion started: 13 May 2025

efficiency of the airflow (approximately 450 m^3/h) ensures the collection of a representative proportion of the aerosols, with a single air filter being sampled within one week from approximately 50,000–100,000 m^3 of pumped air. The temporal scope of the assessment concerned the sampling interval from 2007 to 2021, including the 2011−2013 gap in data collection, during which a considerable number of weekly filters were not available.

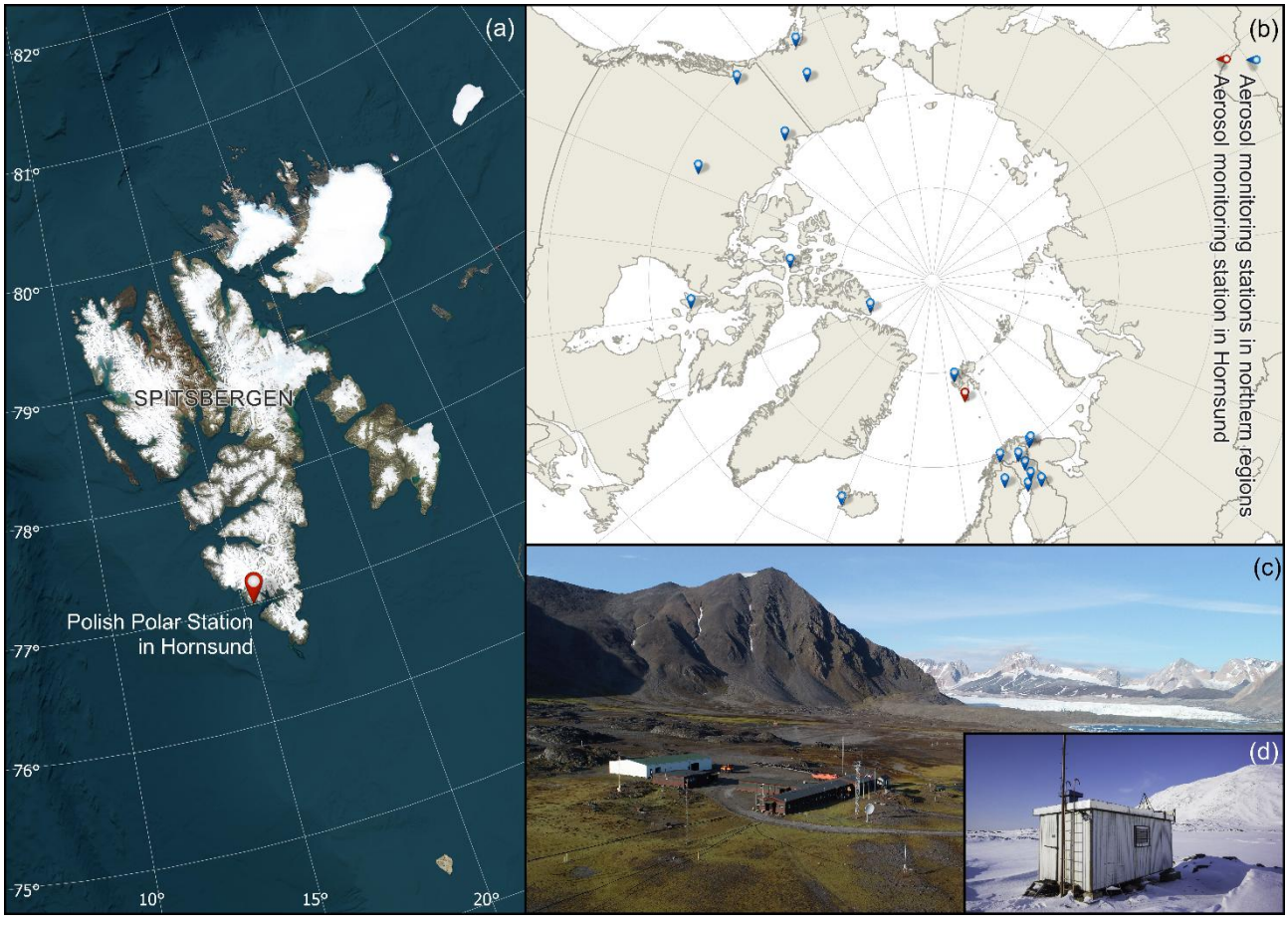

Figure 1: Map of Spitsbergen with position of the sampling station (basemap source: Esri, Maxar, Earthstar Geographics, and the GIS User Community) (a), locations of the air filter sampling stations within the northern regions (b), Stanislaw Siedlecki Polish Polar Station in Hornsund (c) and building with AZA-1000 air sampling system installed in Hornsund (d).

https://doi.org/10.5194/egusphere-2025-1573
Preprint. Discussion started: 13 May 2025

2.2 Meteorological data

Since July 1978, systematic, continuous measurements and observations at World Meteorological Organization (WMO) standards have been conducted at the Hornsund meteorological site (indexed by international numbering system 01003; https://oscar.wmo.int/surface/) (Wawrzyniak and Osuch, 2020). A detailed description of the measurements and instruments at Hornsund station was provided in a collective work edited by Marsz and Styszyńska (2013), while selected information on meteorological variables and current sensors are presented in Table S1.

Svalbard archipelago experiences the highest air temperatures at these latitudes, and the observed climate changes are the largest on Earth (IPCC, 2019). Analysis of the climatological dataset covering 40 years (1978–2018) provides a comprehensive overview of the meteorological conditions in the Hornsund region (Wawrzyniak and Osuch, 2020). The mean annual air temperature is -3.7 °C. The average coldest month is March with a mean air temperature of -10.2 °C, and on average, the warmest month is July with a mean air temperature of 4.6 °C. The influence of the West Spitsbergen Current creates a relatively moist climate, which is reflected in the amount of precipitation, with an annual total reaching 478 mm. In contrast, the interior of Spitsbergen is much drier (200 mm). Winds blowing from the east, along the Hornsund fjord, are prevailing, whereas the wind speed regime is well visible with smaller monthly mean values during summer (minimum 4.0 m/s in June) and larger average values in winter (maximum 7.1 m/s in February). Such variability results from the extreme cyclone events that often occur during Arctic winters (Rinke et al., 2017). The polar night lasts 104 d (31 October–11 February), while the polar day lasts 117 d (24 April–18 August).

This assessment encompassed daily data on air temperature (°C), precipitation (mm), atmospheric pressure (hPa), relative humidity (%), cloudiness (octas), visibility (a.u.), sunshine duration (h), wind speed (m/s) and wind direction (°) collated between 2007 and 2021. For the majority of meteorological parameters, daily mean values were retrieved using the 3-hourly values (eight values a day, between 00:00 and 21:00 UTC), in the case of precipitation 6-hourly values (12:00, 18:00, and 00:00, 06:00 UTC of the following day), and the daily sum of total solar radiation from Campbell–Stokes recorder was obtained at midnight (Wawrzyniak and Osuch, 2020). The wind rose as well as the daily variability of mean air temperature and sum of precipitation for the period of interest are depicted in Figs. 2a, 2c and 2d.

https://doi.org/10.5194/egusphere-2025-1573
Preprint. Discussion started: 13 May 2025

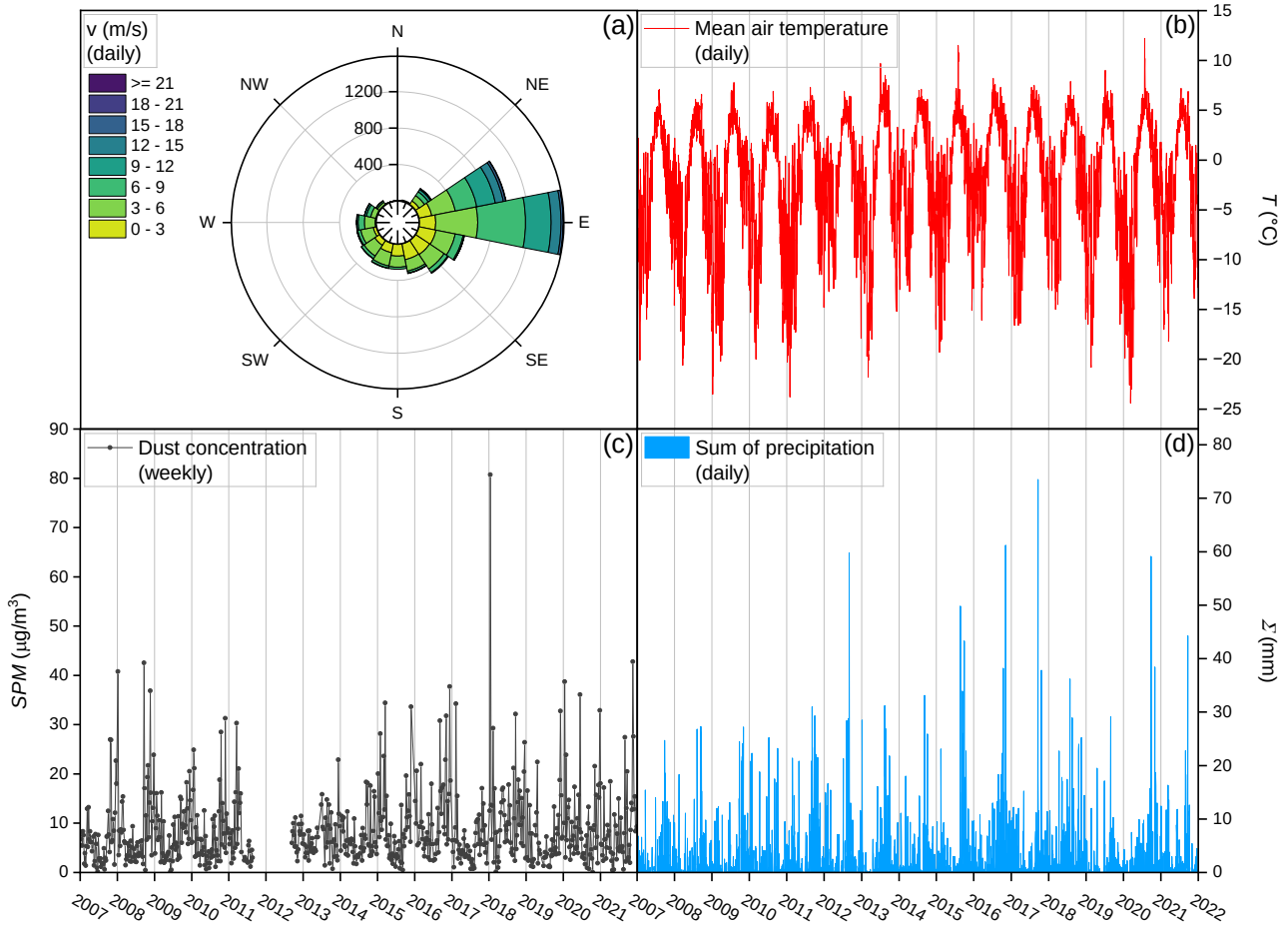

200 **Figure 2: Wind rose (a) according to wind speed (*v*) and wind direction (N, NE, E, SE, S, SW, W, NW) together with variability of mean air temperature (*T*) (b), dust concentration (*SPM*) (c) and sum of precipitation (*Σ*) (d) measured in Hornsund during 2007–2021.**

2.3 Gamma spectrometry measurements

A set of weekly air filters was supplied from the Polish Polar Station in Hornsund, Svalbard archipelago, to the National
205 Center for Nuclear Research (NCBJ) in Świerk, Poland. Before measurement, each sample was subjected to desiccation using halogen infrared heaters (500 W, 220–230 V) to determine the dry mass of the collected dust. Following this, the suspended particulate matter, *SPM*, concentration (µg/m^3) was estimated at week intervals (Fig. 2b). Lastly, all filters were compressed individually to a diameter of 4.5 cm and a thickness of ca. 5 mm. The measurements of gamma-ray spectra were accomplished through a Canberra set comprising HPGe detectors positioned inside low-background shielding chambers with
210 lead-sized walls 10 cm thick. The detector efficiencies range from 35 to 45%, whereas the energy resolutions are between

https://doi.org/10.5194/egusphere-2025-1573
Preprint. Discussion started: 13 May 2025

1.9 and 2.0 keV for 1.33 MeV photons of ^{60}Co. The data acquisition process was facilitated by the Genie-2000 software (Mirion Technologies). The detector efficiency of filter geometry was estimated utilising certified calibration sources with well-known activities. Correction factors were applied to all data to account for decay during sampling time, decay from the end of sampling to the start of measurement, and decay during measurement. The self-absorption correction was found to be negligible due to the minimal height of the samples. The minimum measurable activity concentration for gamma spectrometry, MDC_γ, was estimated according to the Currie law (Currie, 1968). Values of MDC_γ equaled 0.1–1.0 μBq/m³ depending on the radionuclide type. The present study incorporated weekly results on the volume activities (C, μBq/m^3) of ^{7}Be, ^{137}Cs and ^{210}Pb, arranged into time series spanning from 2007 to 2021.

2.4 Radiochemical procedures and alpha spectrometry measurements

The primary phase of the analysis involved the determination of the activity concentrations of ^{238}Pu, $^{239+240}$Pu and ^{241}Am by alpha spectrometry. Given the presumed low quantities of considered alpha emitters over the last two decades in the Hornsund atmosphere, it was hypothesised that the weekly aerosol sample would result in activity concentrations of ^{238}Pu, $^{239+240}$Pu and ^{241}Am not exceeding the minimum measurable activity concentrations for alpha spectrometry, MDC_α. A similar conclusion has been so far formulated by researchers investigating anthropogenic radioisotopes in the ground-level air of European cities during the 21st century (Kierepko et al., 2016; Lujaniene et al., 2012; Nalichowska et al., 2023). Therefore, a set of weekly air filters from Hornsund, corresponding to approximately one-quarter of a year, were aggregated into quarterly samples for the 2007−2010 and 2014−2021 periods. Due to the incomplete collection of weekly filters from 2011 to 2013, only one biennial sample was prepared for the years 2011–2012, while two half-yearly samples were obtained in 2013. The aggregate samples generally consisted of 9–14 weekly filters, with associated total air volumes ranging from 630,000 to 996,319 m^3.

The radiochemical separation of analytes from matrix components (such as organic matter, aeolian dust, anthropogenic particles or filter material) followed the general outline of the method by La Rosa and co-workers in the IAEA Laboratories at Seibersdorf (La Rosa et al., 1992) as well as procedures implemented at the Institute of Nuclear Physics, Polish Academy of Sciences (IFJ PAN) (Mietelski et al., 2000, 2008), which had previously been tested in air filter investigations (Kierepko et al., 2016; Nalichowska et al., 2023). All non-concentrated reagents were prepared by dilution with ultrapure deionised water of Milli-Q®, 18.2 MΩ cm (Merck KGaA). The sample treatment was initiated with the incineration at 600 °C in a muffle furnace. Next, internal tracers of ^{242}Pu (ca. 0.0041 Bq per sample) and ^{243}Am (ca. 0.0077 Bq per sample) were dosed (SRM 4334j and SRM 4332e, respectively, NIST). Near complete sample mineralisation was achieved using concentrated acids (HF, HNO_3 and HCl with H_3BO_3), ending in a filtrated 1M HNO_3 solution. The plutonium fraction was separated from the 8M HNO_3 feed solution via anion exchange with AmberChrom™ 1x8 resin, 100–200 mesh (Sigma-Aldrich), preceded by a Pu(IV) oxidation adjustment procedure. Given the ability of thorium to adsorb on the resin bed, its elution was performed prior to plutonium extraction to prevent potential interference between plutonium and thorium isotopes during alpha spectra acquisition. Pu(IV) was washed out of the resin bed by passing through a mixture of 0.1M HF-0.1M HCl. The

https://doi.org/10.5194/egusphere-2025-1573
Preprint. Discussion started: 13 May 2025

americium analyte, significant quantities of lead, possible traces of thorium, rare earth elements and other matrix impurities were expected to be present in the effluent (8M HNO_3) after the plutonium separation. Experience has shown that the sequential purification steps are necessary for effective extraction and measurement of the americium fraction. The initial removal of lead was achieved by its retention on SR Resin, 100–150 µm of particle size (Triskem International), from the 8M HNO_3 solution. The alkali metals, alkaline earth metals and anionic components were eliminated by subsequent co-precipitation of these elements with calcium oxalate at pH ~ 2.5 and with iron hydroxide(III) at pH ~ 9. Repurification from any residual traces of thorium was then processed using TEVA resin, 100–150 µm of particle size (Triskem International). The Am(III) was separated from the REE and finally eluted by anion-exchange chromatography on AmberChrom™ 1x8 resin, 100–200 mesh, in a methanol-acid medium. Isolated isotopes of Pu and Am were co-precipitated from aqueous solutions with NdF_3 and deposited onto Resolve® filters (Triskem International).

Separation of the interfering analytes of ^{237}Np and ^{242}Pu in a few alpha sources proved essential for further assessment. Hence, a simplified version of the method by La Rosa et al. (2005) was implemented accordingly. In the initial phase, the Pu+Np alpha sources were wet digested with concentrated acid (HCl with H_3BO_3, HNO_3 and $HClO_4$) and subsequently adjusted to the necessary oxidation state (IV). Plutonium and neptunium were separated by ion exchange chromatography utilising AmberChrom™ 1x8 resin, 100–200 mesh. The 8M HNO_3 feed solution was passed through an anion-exchange column in nitrate form, resulting in strong retention of Np(IV) and Pu(IV). Next to the 8M HNO_3 column rinse, the receiver was converted from nitrate to chloride form with 10M HCl. Pu(IV) reduced to Pu(III) was selectively eluted with 0.1M NH_4I-9M HCl, whereas Np(IV) was washed out of the resin bed by passing through a mixture of 0.1M HF-0.1M HCl. The re-preparation of Pu and Np alpha sources involved the procedure mentioned before.

For data acquisition, alpha sources were subjected to vacuum chambers of the AlphaAnalyst™ 7200 spectrometer (Mirion Technologies) close to passivated implanted planar silicon detectors (PIPS®, Mirion Technologies). The PIPS® detector of 450 mm^2 active area has an efficiency of approximately 40%, while the energy resolution is 18 keV for 5.486 MeV alphas of ^{241}Am. All alpha spectra were processed by OriginPro® 2024b software (OriginLab Corporation) using the Peak Analyser tools for baseline correction, peak detection, peak integration or peak fitting. The latter option was applied to resolve the overlapped spectral lines with fitted bigaussian curves. Following the Currie law (Currie 1968), MDC_α values were typically in the range of 0.06 to 0.3 nBq/m^3 for $^{238,\ 239+240}$Pu and ^{241}Am, respectively. The mean percentage of Pu and Am fractions recovered by the chemical process was calculated to be 80.7 ± 2.5% and 43.5 ± 2.2%, respectively. The obtained data set comprised activity concentrations (C, nBq/m^3) of ^{237}Np, $^{238,\ 239+240}$Pu and ^{241}Am, largely determined in quarters for the 2007–2021 period.

2.5 Statistical analysis and modelling

For each radioisotope except ^{237}Np, the basic elements of descriptive statistics were calculated over the years 2007–2021 in accordance with the time intervals at each given radioisotope being measured. This involved the indicating of minimum (min), 25th percentile ($Q1$), median, 75th percentile ($Q3$) and maximum (max) values with interquartile range (IQR), as well

https://doi.org/10.5194/egusphere-2025-1573
Preprint. Discussion started: 13 May 2025

as the estimation of mean and standard deviation (*SD*) parameters. To investigate outliers in the dataset, the interquartile range method of Tukey with multiplier $k = 3$ was employed (Hoaglin 2003). It is critical to note that meteorological indicators, *SPM* factor and gamma emitters were considered as supporting variables to facilitate a thorough evaluation of the annual dynamics of artificial actinides in the lower atmosphere. Consequently, the next stages of statistical analyses necessitated the conversion of daily and weekly parameters into quarterly representation. Data aggregation was performed using the following mathematical methods:

(a) arithmetic mean for daily air temperature, atmospheric pressure, visibility, relative humidity and cloudiness,

(b) sum for daily precipitation and sunshine duration,

(c) magnitude of the resultant wind velocity vector for each of the eight wind sectors (W, E, N, S, NW, NE, SE, SW),

(d) summed activities or masses divided by associated volumes of pumped air in a specific quarter for gamma emitters and *SPM*, respectively.

The input database for calculating Spearman's correlation coefficient (*R*) was constructed by eliminating outliers of radioisotope activity concentrations. Given the non-quarterly character of the data obtained, the 2011–2013 interval was omitted from the correlation matrix of examined alpha emitters against all other variables. The correlation was considered to be statistically significant at a probability level less than or equal to 0.05 ($p \leq 0.05$). Data analysis and visualisation were performed in Python using the following libraries: NumPy, pandas, matplotlib, SciPy and seaborn.

For the reconstruction of radionuclide fate over the explored Arctic region, three-dimensional trajectories of air masses were simulated using the computation model of Hybrid Single-Particle Lagrangian Integrated Trajectory (HYSPLIT) by the National Oceanic and Atmospheric Administration (NOAA, U.S. Department of Commerce). The system offers a range of applications in the domain of propagation and dispersion simulations of forest smoke, hazardous materials, chemicals, and radioactive materials, including the decay of radionuclides in gaseous or particulate forms (Stein et al., 2015). The backward simulations were performed for the assumed point source located at 77°00' N 15°33' E in Hornsund (Fig. 1a). All trajectories have been recreated for archived meteorological data. Quality and robust modelling was facilitated by a simulation grid cell of approximately 2.5° derived from the Climate Data Center (CDC) repository, accessed via the NOAA Air Resources Laboratory (ARL) server.

3 Results and discussion

3.1 Descriptive statistics and time series

This study concerned radionuclides divided into two distinct categories, named herein 'target' and 'background'. The first group comprised subject analytes (^{238}Pu, $^{239+240}$Pu, ^{241}Am), whereas the second group, mostly explained by an earlier study (Burakowska et al., 2021), was used to provide contextual information (^{7}Be, ^{137}Cs, ^{210}Pb). The results of the descriptive statistics analysis are presented in Table 1. Estimating upper limits for outlier values (> *Q3 + 3*IQR*) was a pivotal phase in this assessment, suggesting the potential for radioactive contamination incidents. All values identified as outliers are

https://doi.org/10.5194/egusphere-2025-1573
Preprint. Discussion started: 13 May 2025

distinguished in time series plots (Figs. 3 and 4). The outcomes data have been further plotted in a combined violin and strip charts, allowing a graphical representation of the distribution of probability density for radionuclide activity concentrations (Fig. 5). Since the strip plot arranges points along the x-axis to minimize overlap (and by default, Seaborn adds random jitter to the positioning of the points), it can be observed that some points extend beyond the x-axis range of the violin plot (https://seaborn.pydata.org/). As expected, the naturally occurring radionuclides (^{7}Be, ^{210}Pb) suspended in the lower atmosphere of Hornsund reached higher activity concentrations than the artificial ones (^{137}Cs, ^{238}Pu, $^{239+240}$Pu, ^{241}Am). It was also noted that the mean and median values for each radioisotope individually exhibited significant dispersion, reflected in elevated standard deviations and interquartile ranges (Table 1). Obtained asymmetrical curves pointed to non-normal probability distribution for ^{7}Be, ^{137}Cs, ^{210}Pb, ^{238}Pu, $^{239+240}$Pu and ^{241}Am data (Fig. 5).

Table 1: Descriptive statistics results for activity concentrations of alpha and gamma radioisotopes in aerosol samples collected between 2007 and 2021 in Hornsund, Spitsbergen.

	mean	*SD*	min	*Q1*	median	*Q3*	max	*IQR*	*Q3 + 3*IQR*
^{7}Be (µBq/m^3)	2022	1149	188	1177	1853	2642	8378	1465	7037
^{137}Cs (µBq/m^3)	3.54	28.17	0.07	0.17	0.26	0.45	344.76	0.28	1.28
^{210}Pb (µBq/m^3)	255	249	10	87	163	338	1649	251	1091
$^{239+240}$Pu (nBq/m^3)	1.42	2.55	0.23	0.47	0.77	0.97	15.51	0.50	2.48
^{238}Pu (nBq/m^3)	0.72	1.38	0.02	0.09	0.21	0.59	6.61	0.50	2.09
^{241}Am (nBq/m^3)	31.4	53.3	2.6	11.3	14.9	33.4	353.6	22.1	99.8

3.1.1 Background radioisotopes

Cosmogenic ^{7}Be ($T_{1/2}$ = 53.22 d) is produced in the spallation process of light atomic nuclei (carbon, nitrogen and oxygen) by primary (protons) and secondary (neutrons) particles (Beer et al., 2019). Research by Gaggeler (1995) showed that approximately 67% of ^{7}Be is produced in the stratosphere, with the remaining 33% being produced in the troposphere. It is noteworthy that for the lower atmosphere at mid-latitudes, the ^{7}Be maxima were regularly noticed in late spring (2nd/3rd quarters), coinciding with the most intense exchange process between the stratosphere and the troposphere and subsequent vertical transport through the troposphere (Błażej and Mietelski, 2014; Dueñas et al., 2001; Grossi et al., 2016; Kulan et al., 2006). In contrast, observations for ground-level air of Hornsund (Fig. 3) revealed a ^{7}Be activity concentration peak in early spring (1st/2nd quarters), as reported by previous studies (Burakowska et al., 2021). This was attributed to the reduced vertical mixing of air masses in polar regions, leading to a lower ^{7}Be level in late spring in comparison with temperate zones. The seasonal fluctuations of ^{7}Be in Hornsund were considered to be primarily governed by horizontal tropospheric transfer of haze layers from Eurasian regions that reached higher latitudes during late winter and early spring. Another process that possibly contributed to ^{7}Be variations was wet scavenging, in which radionuclides are washed out of

https://doi.org/10.5194/egusphere-2025-1573
Preprint. Discussion started: 13 May 2025

the atmosphere and deposited on the Earth's surface. Long-term data analysis also confirmed the relationship between the ^{7}Be concentration and the 11-year cycle of solar activity represented by the number of sunspots. The intensity of cosmic radiation has been shown to decrease with increasing solar activity (Beer et al., 2019); thus, the concentration of ^{7}Be in the atmosphere is inversely proportional to the sunspot number. Over the period 2002–2017, examined by Burakowska et al. (2021), the minimal sunspot number per week was reported in 2009–2010, which most likely accounted for two outlier values > 7037 μBq/m^3 of ^{7}Be observed for Hornsund in 2010 (Table 1, Fig. 3).

^{210}Pb ($T_{1/2}$ = 22.3 y) is a radionuclide of terrestrial origin that appears in the uranium-radium series. The presence of ^{210}Pb in the atmosphere is associated with the decay of ^{222}Rn ($T_{1/2}$ = 3.8 d), which has previously been exhaled from the Earth's surface into the atmosphere (Gäggeler, 1995). Grossi et al. (2016) reported that although the ^{210}Pb concentration can increase with altitude and reach high values in the stratosphere over large continental areas, it accumulates mainly in the troposphere. The majority of the ^{210}Pb is present in accumulation mode aerosol particles, which are primarily removed from the atmosphere by precipitation. Despite different origins, the mechanisms behind the behaviour of ^{210}Pb and ^{7}Be in the lower atmosphere were found to be similar for Hornsund, where the annual distribution of ^{210}Pb was only slightly shifted relative to that of ^{7}Be. The elevated levels of ^{210}Pb were identified for the winter months, with the maximum activity concentration occurring in late winter (1st quarter) (Fig. 3). These findings aligned with the results from Ny-Ålesund, Spitsbergen (Paatero et al., 2003, 2010). The ^{210}Pb periodic variations in Hornsund were predominantly influenced by climate patterns and the inflow of air masses of more Arctic origin (possibly continental, from the northern part of Asia or Europe). Outlier values exceeding 1091 μBq/m^3 of ^{210}Pb were observed in 2008, 2009, 2010, 2015, 2019 and 2020 (Table 1, Fig. 3), most likely caused by a reduced sum of precipitation in the listed years (Fig. 2d).

An analysis of fission-produced ^{137}Cs ($T_{1/2}$ = 30.07 y) in ground-level air layers of Hornsund over the years 2007−2021 revealed a median value of 0.26 μBq/m^3. A marked increase of activity concentration, reaching approximately 350 μBq/m^3, was detected in 2011 (Fig. 3). Raised values of ^{137}Cs—persisted in the atmosphere for approximately nine weeks—were linked to the FDNPP failure (AMAP, 2015; Burakowska et al., 2021). This circumstance was indicated as a primary source of outlier values (Table 1, Fig. 3). Additional outliers were identified in 2015 and 2016, yet to a considerably lesser extent and for unknown reasons (Fig. 3). ^{137}Cs activity concentrations in Hornsund surface air were generally consistent with international monitoring results from 2013 to 2020 in the lower atmosphere of the Arctic (Zhang et al., 2022), demonstrating current levels of ^{137}Cs to range from approximately 0.05 to 1.50 μBq/m^3. The likely provenance for this signal was concluded to be resuspension from local soil and re-emission from the combustion of biomass. Periodically increased levels of ^{137}Cs were observed by the daily monitoring stations at Yellowknife, Resolute (62°29′ N, 114°28′ W) and Reykjavik (64°06′ N, 21°54′ W), but not for weekly aerosol filters sampled in Hornsund. In particular, ^{137}Cs peaks manifested at Yellowknife from May until the end of August simultaneously with the wildfire season occurring on an almost yearly frequency (Zhang et al., 2022).

https://doi.org/10.5194/egusphere-2025-1573
Preprint. Discussion started: 13 May 2025

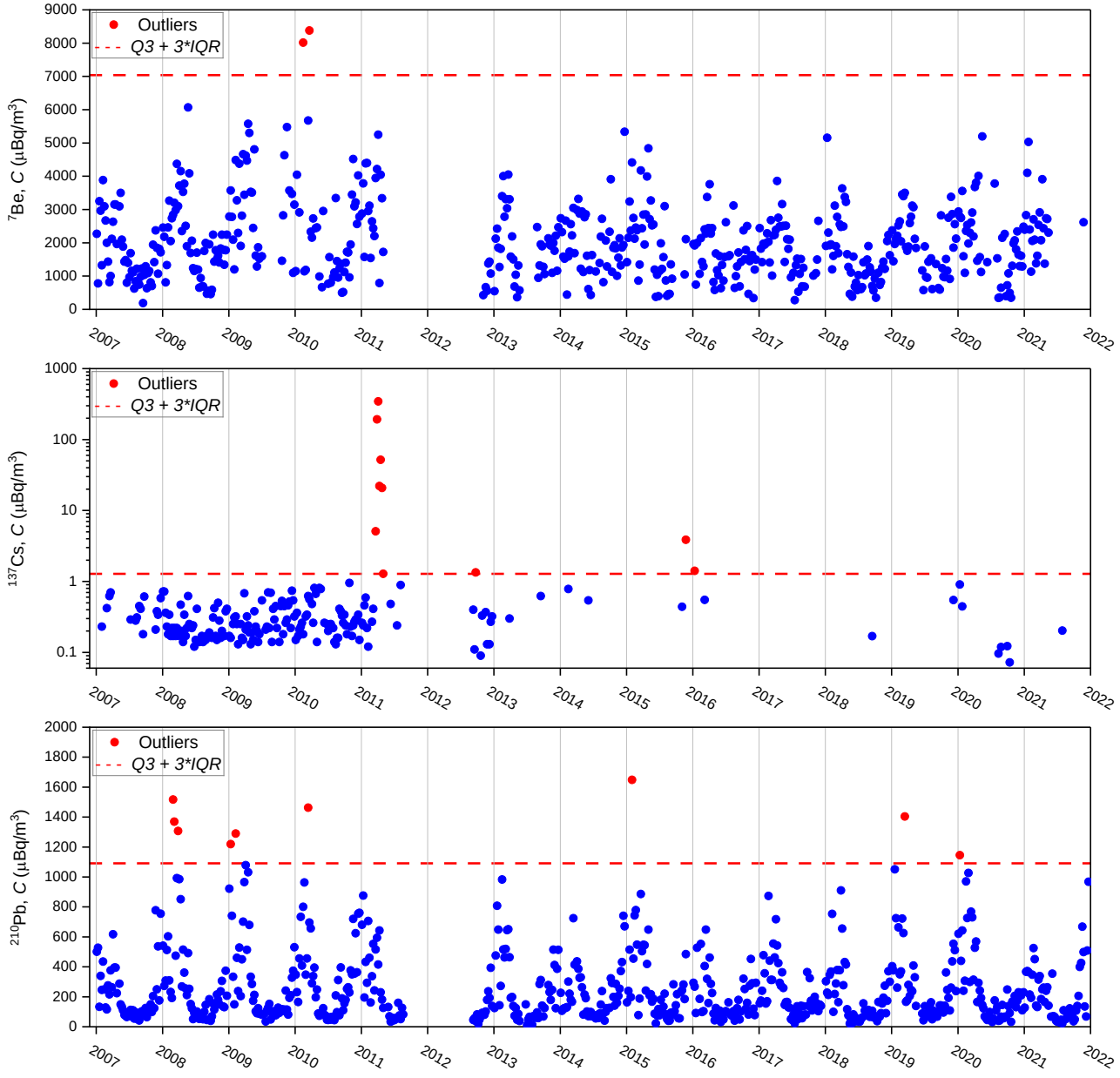

Figure 3: Time series of ^{7}Be, ^{137}Cs and ^{210}Pb activity concentrations (*C*) in weekly air filters collected in Hornsund during 2007–2021; blue dots - non-outlier values, red dots - outlier values.

https://doi.org/10.5194/egusphere-2025-1573
Preprint. Discussion started: 13 May 2025

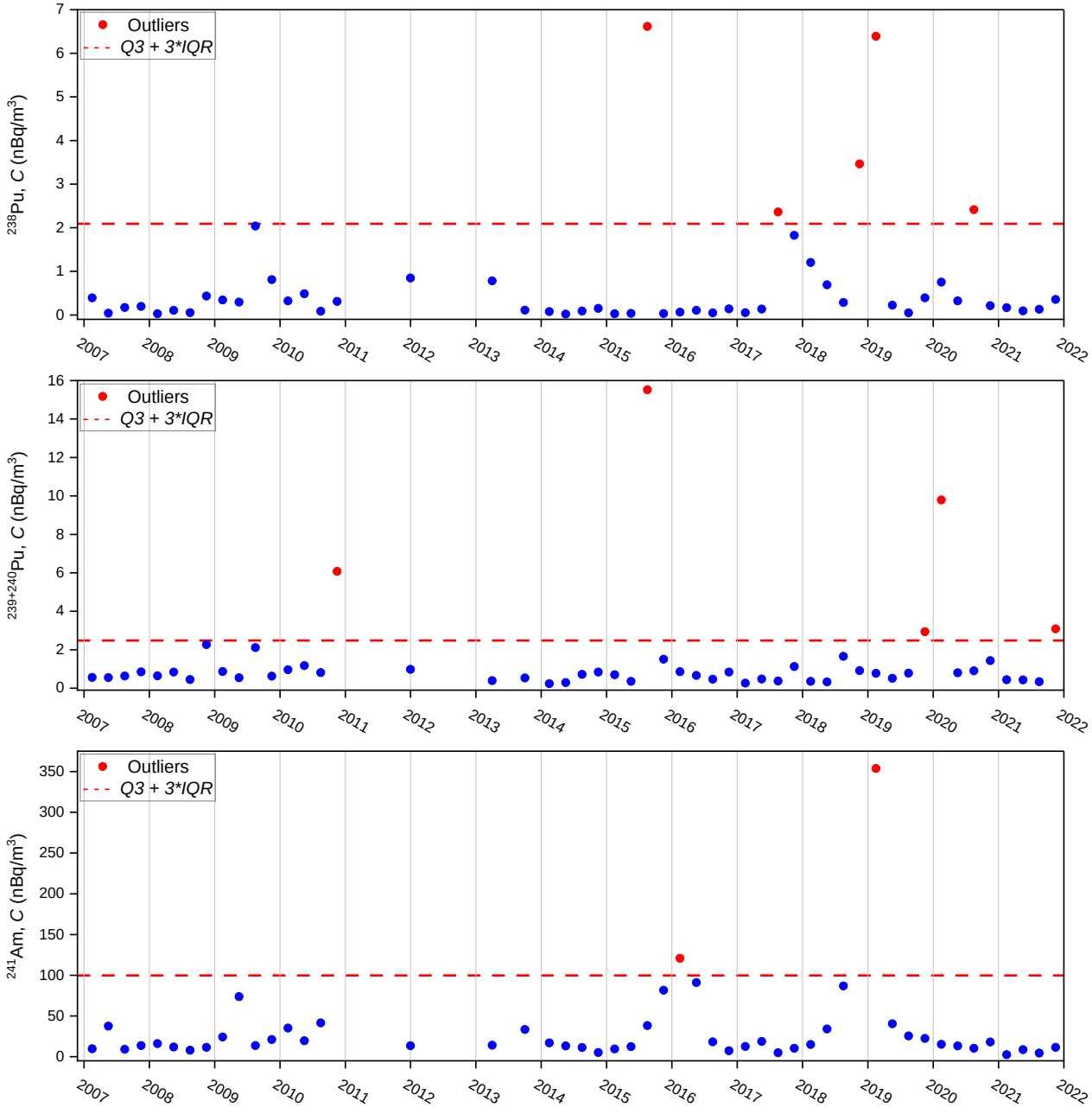

370 **Figure 4: Time series of ^{238}Pu, $^{239+240}$Pu and ^{241}Am activity concentrations (*C*) in quarterly air filters collected in Hornsund during 2007–2021; blue dots - non-outlier values, red dots - outlier values.**

https://doi.org/10.5194/egusphere-2025-1573
Preprint. Discussion started: 13 May 2025

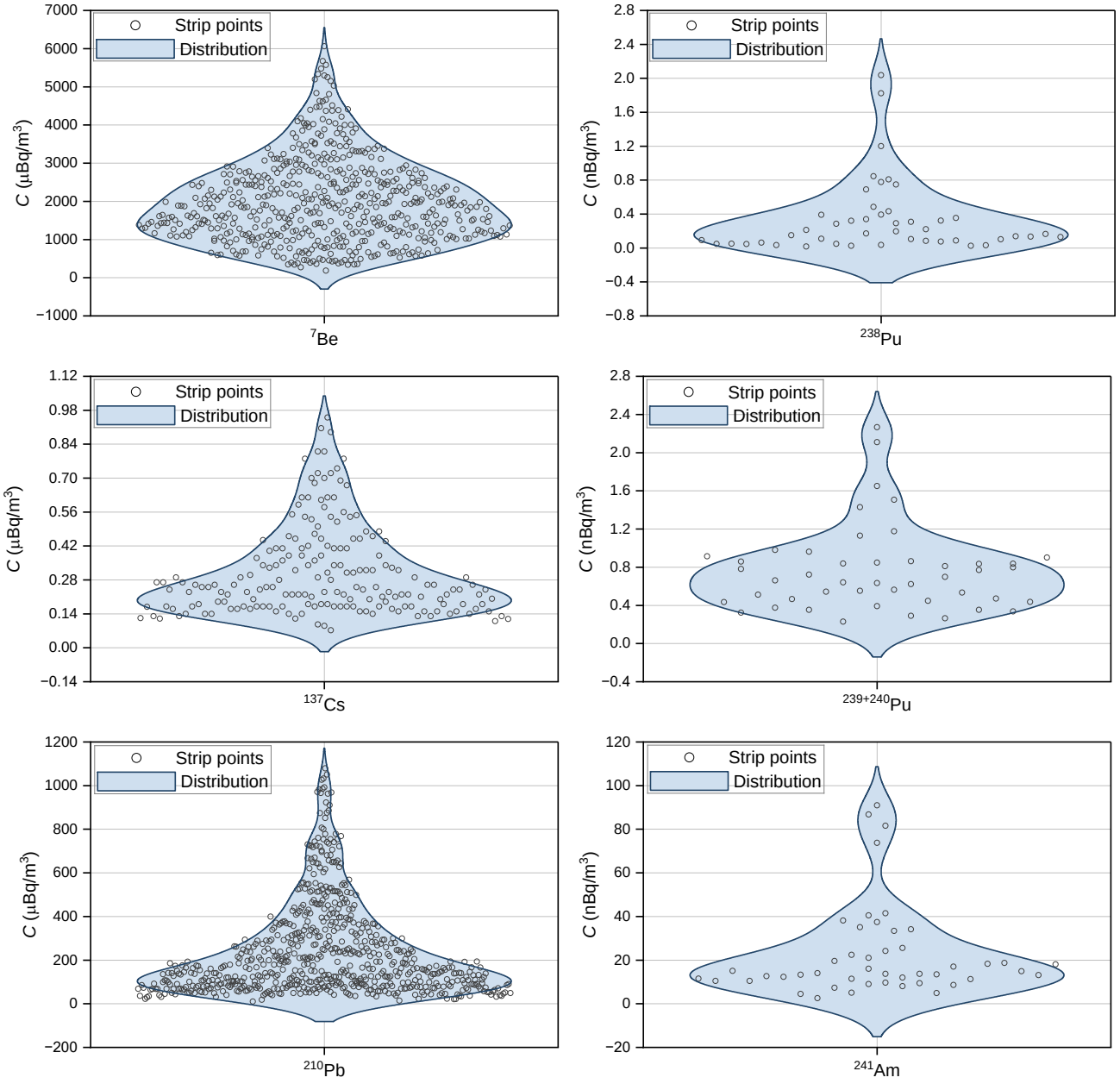

Figure 5: Combined violin and strip plots of ^{7}Be, ^{137}Cs, ^{210}Pb ^{238}Pu, $^{239+240}$Pu and ^{241}Am activity concentrations (*C*) in weekly or quarterly air filters collected in Hornsund during 2007–2021.

https://doi.org/10.5194/egusphere-2025-1573
Preprint. Discussion started: 13 May 2025

3.1.2 Target radioisotopes

A thorough analysis of the time series for artificial alpha emitters of ^{238}Pu, $^{239+240}$Pu and ^{241}Am suspended in Hornsund surface air spanning 2007−2021 showed that annual regularities could not be easily identified (Fig. 4). The highest activity concentrations of 6.61 nBq/m^3 for ^{238}Pu and 15.51 nBq/m^3 for $^{239+240}$Pu occurred in the 3rd quarter of 2015, whereas the maximum of 353.6 nBq/m^3 for ^{241}Am was noted in the 1st quarter of 2019 (Fig. 4). Additional peaks were observed in the following years: 2009, 2017, 2019 and 2020 for ^{283}Pu, 2010 and 2020 for $^{239+240}$Pu along with 2016 for ^{241}Am (Fig. 4). These elevated values were classified as outliers in the majority of cases (Table 1). The examples of alpha spectra representing deviated activity concentrations of $^{238, 239+240}$Pu in 2015 and ^{241}Am in 2016 are illustrated by Fig. S1. The median values (Table 1) of ^{238}Pu and $^{239+240}$Pu (0.21 nBq/m^3 and 0.77 nBq/m^3, respectively) were found to be approximately two or three orders of magnitude lower than those of ^{241}Am and ^{137}Cs (14.9 nBq/m^3 and 260 nBq/m^3, respectively). The distinct enhancement of ^{137}Cs to $^{239+240}$Pu and ^{238}Pu was expected, given that previous nuclear events had released at least a tenfold higher activity of ^{137}Cs than $^{239+240}$Pu, ^{241}Am or ^{238}Pu (UNSCEAR, 1993, 2000a, b). However, a particular challenge was encountered in explaining the results from Hornsund, where the median of ^{241}Am was notably larger than that of $^{239+240}$Pu (Table 1). Potential reasons for the observed dynamics of changes and isotopic compositions of artificial actinides in ground-level air of Hornsund for 2007–2021 required further analyses, to be discussed in the following sections.

Plutonium and americium isotopes were recorded at other sampling sites during the 21st century. Nalichowska et al. (2023) studied the dynamics of changes of ^{238}Pu and $^{239+240}$Pu in monthly air filter samples for the 2010–2016 interval in Kraków, Poland (50°04′ N, 19°58′ W), which partly covered the years 2007–2021 of the present assessment. The activity concentrations measured in Kraków averaged 2.07 nBq/m^3 for $^{239+240}$Pu and 0.15 nBq/m^3 for ^{238}Pu, consistent with the mean values reported in Hornsund (Table 1). Moreover, the highest activity concentrations of 1.27 nBq/m^3 for ^{238}Pu and 13.1 nBq/m^3 for $^{239+240}$Pu were detected in the 1st and 3rd quarter of 2015, respectively. The surface air in Vilnius, Lithuania (54°42′ N, 25°30′ E) exhibited one order of magnitude higher level of $^{239+240}$Pu, with a range of 0.9–300 nBq/m^3 and a mean activity concentration of 13.4 nBq/m^3 in monthly samples acquired for the 1995–2011 period (Lujaniene et al., 2012). The ^{241}Am values varied from 0.32 to 25 nBq/m^3 and averaged 4.3 nBq/m^3 in 2005–2006, indicating an order of magnitude lower level than that observed at the Hornsund station (Table 1). The Preila sampling station (55°20′ N, 21°00′ E), situated 300 km from Vilnius, revealed $^{239+240}$Pu levels ranging from 1 to 16 nBq/m^3, with a mean of 6.2 nBq/m^3 for the 1995–1999 interval (Lujaniene et al., 2012). The disparities between the Preila and Vilnius data sets were ascribed to the sampling conditions. The Preila sampling station is situated at the Curonian Split on the seashore, where prevailing winds from the Baltic Sea are expected to result in reduced radionuclide contributions from soil resuspension and the Chernobyl contaminated zone when compared to the Vilnius station (Lujaniene et al., 2012). Furthermore, a recent study of the urban air in Lodz, Poland (51°48′ N, 19°30′ E), identified ^{241}Am signal over seven weeks from April to June 2021 using weekly aerosol filters (Długosz-Lisiecka and Isajenko, 2024). The results showed a change between 305 and 4241 nBq/m^3. During the same

https://doi.org/10.5194/egusphere-2025-1573
Preprint. Discussion started: 13 May 2025

period, a decrease in the activity concentrations of ^{241}Am to several nBq/m^3 was noticed in the ground-level air layers of Hornsund.

In the context of the Arctic region, data concerning ^{238}Pu, $^{239+240}$Pu and ^{241}Am in the lower atmosphere from most northerly areas during the 21st century cannot be found. The primary focus of air sampling stations mapped in Fig. 2b is constrained to the determination of primarily ^{7}Be, ^{133}Xe, ^{137}Cs and ^{210}Pb (+ ^{90}Sr controlled at sites in northern Russia; not included in Fig. 2b) (AMAP, 2002, 2009, 2015). The present investigation is, therefore, the sole radioactivity monitoring that has yielded long-term results on artificial actinides for the Arctic region in the recent two decades. The earlier analogous assessment, encompassing sites proximate to and above the Arctic Circle, was facilitated by the NRL measurements between 1957 and 1962, followed by the EML SASP continuation from 1963 to 1999 (Larsen et al. 1995). The time series of ^{137}Cs and $^{239+240}$Pu for surface aerosol samples collected by stations north of 50° N (Kap Tobin, Constable Point, Thule and Nord in Greenland; Barrow in Alaska, USA; Moosonee in Ontario, Canada; Bravo Ocean Station; Charlie Ocean Station) are depicted in Fig. S2. The provided database offered a quantitative perspective on the temporal dynamics of anthropogenic radionuclides. It has been documented that during the most intense phase of atmospheric nuclear testing (the 1960s), ^{137}Cs and $^{239+240}$Pu levels were as high as a few or several thousand µBq/m^3 and nBq/m^3, respectively (Fig. S2). This trend ceased by the 1980s, once global fallout became negligible, allowing specific contamination from local nuclear accidents and resuspension processes of Cs- and Pu-bearing particles to dominate (Chamizo et al., 2010). For instance, the elevated activity concentrations of ^{137}Cs noted in 1986 were attributed to local post-Chernobyl fallout (Larsen et al. 1989) (Fig. S2). The level of suspended traces of ^{137}Cs and $^{239+240}$Pu at locations north of 50° N in the late 1980s and 1990s aligned with 21st-century data from the Hornsund region (Fig. S2, Figs. 3 and 4).

3.2 ^{237}Np incidents

The chemical protocol applied in this study was founded on the premise that neptunium occurs at a level that falls below the detection limits of alpha spectrometry. The common practice for the majority of environmental samples is grounded in the observation that the deposited activity of ^{237}Np ($T_{1/2}$ = 2.144 10^6 y) is approximately three orders of magnitude lower than that of ^{239}Pu activity, as estimated by Kelley et al. (1999) for global fallout. Along with the plutonium elution, neptunium is removed from the resin bed; however, no issues are usually encountered during subsequent measurements. Analyses of three collective samples from Hornsund unexpectedly revealed a distinct signal of ^{237}Np, which partially overlapped with the ^{242}Pu peak as exampled in Fig. S3 (Pu+Np). The ^{237}Np was identified in the 2nd half of 2013, 1st quarter of 2014 and 4th quarter of 2018. These findings have necessitated additional evaluation. Therefore, Pu+Np analytes were separated by approach unequivocally confirming the presence of ^{237}Np in suspected samples, illustrated by Fig. S3 (Pu, Np). In a quantitative assessment, the overlapped peaks of ^{237}Np and ^{242}Pu were used to selectively integrate the counts after fitting bigaussian curves (Fig. S4). Assuming ^{242}Pu-based chemical recovery for ^{237}Np fraction (Qiao et al., 2010, 2013), the activity concentrations of ^{237}Np were estimated to be 14.03 ± 0.66 nBq/m^3 in the 2nd half of 2013, 4.22 ± 0.29 nBq/m^3 in the

https://doi.org/10.5194/egusphere-2025-1573
Preprint. Discussion started: 13 May 2025

1st quarter of 2014 and 7.39 ± 0.25 nBq/m^3 in the 4th quarter of 2018. The ^{237}Np incident was found to be correlated with an increased level of ^{238}Pu solely during the 4th quarter of 2018.

The ^{237}Np signal was not detected in aerosol sample investigations in Krakow or Vilnius, based on the radiochemical procedures with no step dedicated to separate plutonium and neptunium fraction (Lujaniene et al., 2012; Nalichowska et al., 2023). This prompted us to perform in-depth analyses of the blank samples, controlling not only the reagents used but also the filter material and equipment in direct contact with the aerosol sample. One type of blank sample comprised solely of the procedural reagents (designated 'blank'), while the second type was a simulated collective sample consisting of 12 cleanly pressed Petrianov filters (designated 'blank filter'). The presence of the radioisotopes in aerosol samples was not caused by laboratory contamination or contamination of a spectrometric unit (Table S2). Further quality control was performed on the reference materials IAEA-447 and IAEA-385, with the determined activity concentrations of target ^{238}Pu, $^{239+240}$Pu and ^{241}Am radionuclides. The experimental results were found to align with the certified values (Table S3).

3.3 Correlation and seasonality evaluation

A quarterly correlation assessment was a relevant component of the investigation into the temporally changing activity concentrations of the studied radioisotopes in the Hornsund lower atmosphere. Spearman's correlation coefficient was selected to minimise the influence of outliers and account for the non-normal distribution of the data (Mukaka, 2012; Schober and Schwarte, 2018) (Fig. 5). The obtained results are given in Tables 2, 3 and 4. Statistically significant items ($p \leq 0.05$) are indicated by asterisks (*). Additionally, moderate and strong linkages between variables ($|R| \geq 0.4$) are denoted in bold. The input database used for calculating the correlation matrix is shown in Tables S4 and S5.

The mutual correlations of radionuclides with meteorological parameters were at least moderate or strong for ^{7}Be, ^{210}Pb vs. air temperature, the sum of precipitation, relative humidity, cloudiness, eastern (E) and northeastern (NE) winds; the latter only for ^{210}Pb (Table 2). The negative monotonic tendency manifested among ^{7}Be, ^{210}Pb and air temperature, precipitation, relative humidity, cloudiness, yet a positive monotonic trend emerged for ^{7}Be, ^{210}Pb and E, NE wind directions. Weak anticorrelation was reported for ^{7}Be, ^{210}Pb vs. southern (S) winds along with ^{210}Pb vs. sunshine duration, southeastern (SE) winds, whereas no correlation was noted between ^{7}Be, ^{210}Pb and *SPM* factor (Table 3). The findings corroborated the hypothesis concerning the transportation and behaviour of ^{7}Be and ^{210}Pb in Hornsund surface air, which were blown in by the prevailing easterly winds and scavenged by precipitation. Furthermore, the quarterly resolution proved suitable for the recognition of relationships concerning climatic factors and natural radioisotopes. The ^{137}Cs case appears excessively questionable to interpret at this point, given the large number of weekly results falling below the detection limit since 2013 (Fig. 3). Artificial radioisotopes suspended in ground-level air of Hornsund between 2007 and 2021 exhibited no statistically significant response to the prevailing climatic conditions, except for $^{239+240}$Pu vs. sunshine duration (Table 2). The subsequent evaluation demonstrated a positive but rather weak correlation between $^{239+240}$Pu and *SPM* parameter (Table 3). To a certain extent, the *SPM* contribution evidenced a terrestrial origin of $^{239+240}$Pu, attributable more to local resuspension and shallow transfer towards the sampling site. The dust concentration typically reached a maximum in the 1st and

https://doi.org/10.5194/egusphere-2025-1573
Preprint. Discussion started: 13 May 2025

4th quarters (Fig. 2b, Table S5), likely as a result of the extreme cyclone events that often occur during Arctic winters (Wawrzyniak and Osuch, 2020). Therefore, $^{239+240}$Pu displayed a tendency to be elevated in polar night months and reduced in polar day months, clarifying the weak negative correlation with sunshine duration.

475

Table 2: Mutual correlations of the radioisotope activity concentration and selected meteorological indicators.

	^{7}Be		^{137}Cs		^{210}Pb		$^{239+240}$Pu		^{238}Pu		^{241}Am	
	R	***p***	***R***	***p***	***R***	***p***	***R***	***p***	***R***	***p***	***R***	***p***
Air temperature	**-0.61***	**0.00**	-0.21	0.25	**-0.90***	**0.00**	-0.03	0.84	-0.16	0.29	-0.02	0.92
Precipitation	**-0.47***	**0.00**	-0.27	0.14	**-0.48***	**0.00**	0.18	0.24	-0.03	0.87	-0.11	0.50
Air humidity	**-0.41***	**0.00**	-0.29	0.11	**-0.75***	**0.00**	0.10	0.52	-0.22	0.16	0.01	0.97
Cloudiness	**-0.52***	**0.00**	-0.09	0.64	**-0.80***	**0.00**	-0.01	0.97	-0.23	0.14	0.00	0.99
Sunshine duration	0.08	0.58	-0.08	0.67	-0.32*	0.01	-0.38*	0.01	-0.20	0.19	0.23	0.13
Visibility	0.10	0.47	-0.16	0.39	-0.12	0.39	-0.20	0.20	0.08	0.63	0.22	0.15
Air pressure	0.01	0.96	-0.17	0.37	-0.23	0.09	-0.27	0.08	0.01	0.94	0.27	0.08
N	0.00	0.97	0.22	0.22	0.11	0.43	0.12	0.43	-0.14	0.38	-	-
NE	0.26	0.06	0.27	0.14	**0.57***	**0.00**	0.30	0.05	0.29	0.06	-0.14	0.37
E	**0.46***	**0.00**	0.21	0.25	**0.55***	**0.00**	0.25	0.10	0.29	0.06	-0.03	0.83
SE	-0.16	0.25	0.19	0.31	-0.28*	0.03	-0.08	0.60	-0.20	0.20	0.04	0.80
S	-0.35*	0.01	-0.23	0.21	-0.35*	0.01	0.10	0.54	-0.17	0.27	0.11	0.47
SW	-0.08	0.55	-0.15	0.40	-0.13	0.32	-0.13	0.39	-0.17	0.27	-0.11	0.47
W	-0.13	0.33	-0.08	0.68	-0.15	0.27	-0.16	0.31	-0.18	0.26	-0.16	0.31
NW	0.22	0.12	-0.11	0.57	0.18	0.19	-0.13	0.41	-0.13	0.39	0.11	0.49

* $p \leq 0.05$

Table 3: Mutual correlations of the radioisotope activity concentration and *SPM*.

	***SPM* concentration**	
	R	***p***
$^{239+240}$Pu	0.32*	0.04
^{238}Pu	0.23	0.13
^{241}Am	-0.05	0.73
^{7}Be	0.06	0.67
^{137}Cs	0.05	0.77
^{210}Pb	0.23	0.08

* $p \leq 0.05$

https://doi.org/10.5194/egusphere-2025-1573
Preprint. Discussion started: 13 May 2025

480 **Table 4: Total and seasonal cross-correlations of radioisotope activity concentrations.**

total	**^{238}Pu**		**^{241}Am**		**^{7}Be**		**^{137}Cs**		**^{210}Pb**	
	R	***p***	***R***	***p***	***R***	***p***	***R***	***p***	***R***	***p***
$^{239+240}$Pu	0.33*	0.04	0.20	0.21	-0.21	0.19	-0.19	0.41	-0.08	0.63
^{238}Pu	1.00		0.05	0.76	0.13	0.42	0.10	0.64	0.08	0.59
^{241}Am			1.00		-0.01	0.95	0.05	0.84	0.05	0.71
^{7}Be					1.00		0.20	0.30	**0.78***	**0.00**
^{137}Cs							1.00		0.25	0.17
1st quarter	**^{238}Pu**		**^{241}Am**		**^{7}Be**		**^{137}Cs**		**^{210}Pb**	
	R	***p***	***R***	***p***	***R***	***p***	***R***	***p***	***R***	***p***
$^{239+240}$Pu	0.01	0.99	0.32	0.41	**0.62***	**0.04**	-0.60	0.21	**0.72***	**0.01**
^{238}Pu	1.00		0.16	0.65	0.06	0.85	0.14	0.76	0.07	0.83
^{241}Am			1.00		0.39	0.26	-0.37	0.47	0.39	0.26
^{7}Be					1.00		**-0.78***	**0.01**	**0.56***	**0.04**
^{137}Cs							1.00		-0.29	0.44
2nd quarter	**^{238}Pu**		**^{241}Am**		**^{7}Be**		**^{137}Cs**		**^{210}Pb**	
	R	***p***	***R***	***p***	***R***	***p***	***R***	***p***	***R***	***p***
$^{239+240}$Pu	0.37	0.24	0.14	0.66	0.22	0.5	-0.20	0.80	-0.08	0.81
^{238}Pu	1.00		0.29	0.37	-0.01	0.97	-0.40	0.60	-0.19	0.56
^{241}Am			1.00		-0.39	0.21	-0.40	0.60	-0.17	0.60
^{7}Be					1.00		-0.50	0.39	**0.67***	**0.01**
^{137}Cs							1.00		-0.60	0.28
3rd quarter	**^{238}Pu**		**^{241}Am**		**^{7}Be**		**^{137}Cs**		**^{210}Pb**	
	R	***p***	***R***	***p***	***R***	***p***	***R***	***p***	***R***	***p***
$^{239+240}$Pu	0.47	0.21	**0.74***	**0.01**	0.37	0.29	0.07	0.88	0.25	0.47
^{238}Pu	1.00		-0.05	0.9	-0.07	0.87	0.37	0.47	-0.32	0.41
^{241}Am			1.00		0.22	0.52	-0.04	0.94	0.52	0.08
^{7}Be					1.00		0.43	0.34	0.45	0.14
^{137}Cs							1.00		0.20	0.58
4th quarter	**^{238}Pu**		**^{241}Am**		**^{7}Be**		**^{137}Cs**		**^{210}Pb**	
	R	***p***	***R***	***p***	***R***	***p***	***R***	***p***	***R***	***p***
$^{239+240}$Pu	-0.05	0.91	0.29	0.49	-0.28	0.46	-0.10	0.87	-0.60	0.09

https://doi.org/10.5194/egusphere-2025-1573
Preprint. Discussion started: 13 May 2025

^{238}Pu	1.00		0.01	0.99	0.53	0.10	-0.21	0.64	-0.21	0.54
^{241}Am			1.00		-0.09	0.80	0.66	0.16	-0.07	0.85
^{7}Be					1.00		0.19	0.65	**0.71***	**0.00**
^{137}Cs							1.00		0.62	0.10

* $p \leq 0.05$

The next phase of investigations focused on cross-correlations among specific radionuclides parallel to the median and mean activity concentrations assessment within designated quarters. The results obtained are presented in Table 4 and illustrated by Fig. 6. Positive strong correlations for natural radionuclides were exhibited in both the total and seasonal dataset, particularly during the 1st, 2nd and 4th quarters (Table 4). Highly consistent temporal dynamics of changes for ^{7}Be and ^{210}Pb in the Hornsund atmosphere were also reflected by the seasonal median trends (Fig. 6). Strong correlations were obtained for artificial radioisotopes during the 1st quarter in the case of $^{239+240}$Pu vs. ^{7}Be, $^{239+240}$Pu vs. ^{210}Pb and ^{137}Cs vs. ^{7}Be as well as during the 3rd quarter between $^{239+240}$Pu and ^{241}Am. All highlighted tendencies manifested as positively monotonic, with the exception of ^{137}Cs vs. ^{7}Be. Most likely, horizontal air mass movement played a significant role in the transportation of $^{239+240}$Pu along with ^{7}Be and ^{210}Pb during the 1st quarter. A similar pattern of supply may have also accounted for the linkage between ^{241}Am and $^{239+240}$Pu in the 3rd quarter. A weak relationship for $^{239+240}$Pu and ^{238}Pu could only be established for the cumulated dataset, i.e. incorporating all quarters in the calculation. The aforementioned observation was also supported by comparable annual fluctuations of the median values for ^{238}Pu and $^{239+240}$Pu. Generally, higher median values were observed in the 4th quarter for ^{137}Cs, ^{238}Pu and $^{239+240}$Pu and in the 2nd quarter for ^{241}Am, whilst the lower median levels were recorded in the 2nd quarter for ^{238}Pu and $^{239+240}$Pu, in the 3rd quarter for ^{137}Cs, and in the 3rd/4th quarters for ^{241}Am.

The analysis of $^{239+240}$Pu time-series for air filters from Krakow in 2010−2016 demonstrated clear periodic fluctuations of $^{239+240}$Pu from maximum activity concentrations observed in the spring and summer to minimum activity concentrations in the autumn and winter (Nalichowska et al., 2023). Moreover, the mutual correlation evaluation between the $^{239+240}$Pu and meteorological indicators unveiled the dependence on specific weather conditions, including wind strength, the activity of atmospheric fronts, precipitation, cloudiness, humidity and air temperature, but no *SPM* factor. The results suggest that $^{239+240}$Pu in Krakow was predominantly blown in and wet-scavenged rather than being resuspended locally, whereas, in Hornsund, the scenario was likely the reverse. An analogous interpretation of the data was proposed by Lujaniene et al. (2012) for Vilnius air filters. As reported, there was no relationship between *SPM* and $^{239+240}$Pu activity concentration in the years 1995−1999, however, a significant correlation was obtained for the 2005−2006 period ($R = 0.83$, $p < 0.01$). The latter observation was treated as evidence for a terrestrial origin of in situ redistributed dust particles, a conclusion also drawn for $^{239+240}$Pu during the entire 2007−2021 monitoring in ground-level air layers of Hornsund.

https://doi.org/10.5194/egusphere-2025-1573
Preprint. Discussion started: 13 May 2025

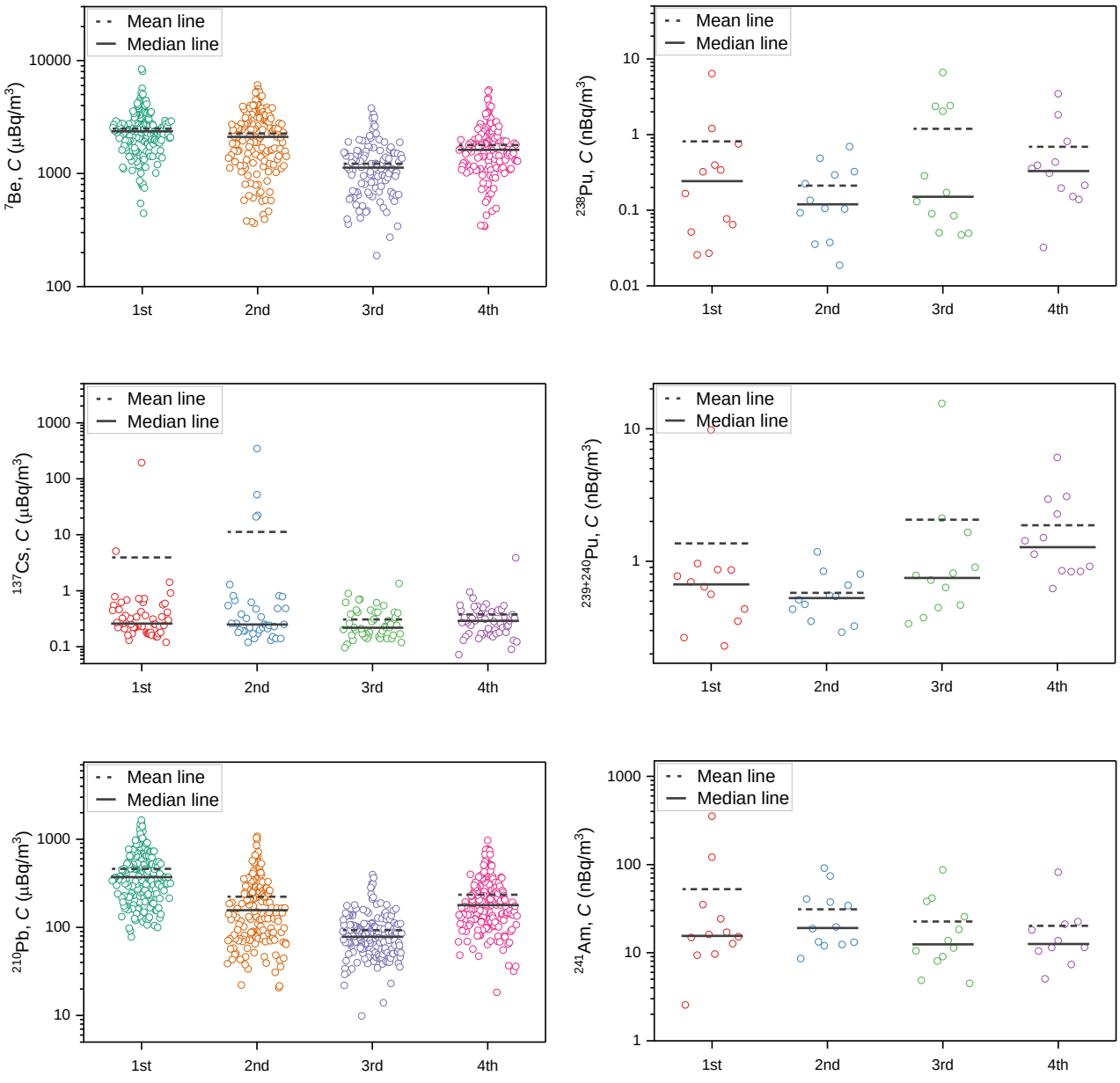

Figure 6: Descriptive statistics in quarters (1st, 2nd, 3rd, 4th) for ^{7}Be, ^{137}Cs, ^{210}Pb, ^{238}Pu, $^{239+240}$Pu and ^{241}Am activity concentrations (*C*) in weekly or quarterly air filters collected from Hornsund during 2007–2021.

https://doi.org/10.5194/egusphere-2025-1573
Preprint. Discussion started: 13 May 2025

3.4 Potential origin of radioactive contamination

The activity ratios (*IR*) of artificial actinides were investigated to infer their provenance (Table S7, Fig. 7), taking into account reference signatures for specific nuclear events given in Table S6. These ratios are known to vary with reactor type, neutron flux and energy, nuclear fuel burn-up time or, for fallout from nuclear detonations, bomb type and yield (Oughton et al., 2001). Typically, $^{238}Pu/^{239+240}Pu$ (and $^{241}Am/^{239+240}Pu$) isotopic compositions (Table S6) in nuclear reactors (NPP) and fuel reprocessing plants (NRP) are about an order of magnitude greater than for global fallout (GF) or isotopic production grade (PPP).

The $^{238}Pu/^{239+240}Pu$ values varied from 0.021 to 8.3, whereas $^{241}Am/^{239+240}Pu$ results ranged between 1.5 and 460 in Hornsund surface air (Table S7). Noteworthy, both maxima were found in the 1st quarter of 2019, shortly after the ^{237}Np incident occurred. The $^{238}Pu/^{239+240}Pu$ ratios demonstrated a large diversity over the entire controlled period, mostly ranging between the reference limits typical for GF (+ SNAP 9A) and Chernobyl fallout (Table S7, Fig. 7). Considering only the literature data (Table S6), these results indicated a mixing of the global fallout (+ SNAP 9A) and releases from nuclear power plants or nuclear reprocessing plants. Besides, only one point was consistent with the GF (+ SNAP 9A) isotopic composition, while several points in 2009–2013 and 2017–2020 presented $^{238}Pu/^{239+240}Pu$ ratios noticeably above the known reference signatures (Table S6). The latter outcome manifested as a persistent feature in the $^{241}Am/^{239+240}Pu$ data, exhibiting an unprecedented enhancement of ^{241}Am with respect to established ratios for prior nuclear releases (Fig. 7, Table S6).

Generally, radioactive contamination of the Arctic has occurred at two different scales (AMAP, 2002, 2009):

(a) widespread contamination associated with global nuclear weapons testing (88 of these have taken place in the Arctic test site of Novaya Zemlya), Sellafield and Cap La Hague releases and the Chernobyl or Fukushima accidents,

(b) localized contamination of smaller areas resulting, for instance, from the Thule nuclear weapons accident and radioactive wastes dumped at sea in the vicinity of Novaya Zemlya (e.g. Abrosimov Fjord, Stepovogo Fjord).

The presence of plutonium and americium fallout from nuclear weapon tests has been well documented in the Spitsbergen region, whereas no such influence has been demonstrated for the Chernobyl, Fukushima or Thule releases at the time of injection (Eriksson et al., 2004; Gwynn et al., 2004; Łokas et al., 2013, 2017b). Nevertheless, the elevated $^{238}Pu/^{239+240}Pu$ ratios in cryoconite collected in 2011 from Hans Glaciers, located on the northern coast of Hornsund, indicated likely contributions from plutonium sources other than global fallout (Łokas et al., 2016). The highest recorded value of $^{238}Pu/^{239+240}Pu$ reached 0.118 ± 0.017. Additionally, the $^{241}Am/^{239+240}Pu$ ratios of the Spitsbergen environment were determined for soils and lake sediments in the central part, as well as proglacial and tundra soils from the southwestern part, collected in 2007 and 2005, respectively (Łokas et al., 2017b, a). The obtained results varied in soils and sediments from 0.18 to 1.05 and for proglacial soils from 0.18 to 0.88. The maximum values represented raised levels of $^{241}Am/^{239+240}Pu$ with respect to the GF level. Although data for soil, sediment or cryoconite are valuable, there is a substantial difference between these types of samples and air filter samples. The first group reports on averaged contamination accumulated for at least several years, whereas the second group provides information on the dynamics of changes in airborne contaminants over a

https://doi.org/10.5194/egusphere-2025-1573
Preprint. Discussion started: 13 May 2025

relatively short period of time (day, week, quarter). Furthermore, samples accumulated over a few decades are affected by the prominent presence of signals from nuclear weapons testing, which limits the ability to detect traces of artificial radionuclides from other sources. Consequently, comparing isotopic ratios between these two types of samples is problematic and should be treated as a premise for a given interpretation rather than as strong evidence. ^{238}Pu and ^{241}Am enrichment in soil, sediment and cryoconite may be linked to high values of ^{238}Pu/$^{239+240}$Pu and ^{241}Am/$^{239+240}$Pu for nuclear aerosols but cannot report on the exact magnitude of isotopic ratios in the atmosphere.

A long-term study of ^{238}Pu/$^{239+240}$Pu activity ratios in air filters from Poland documented the highest values of 33.7 ± 3.6 in the 1st quarter of 2000 for Bialystok and 1.29 ± 0.25 in the 1st quarter of 2002 for Krakow (Kierepko et al., 2016). Besides, two decades of research on radioactivity in the surface air of Poland between the 20th and 21st centuries typically yielded results of ^{238}Pu/$^{239+240}$Pu indicating a mixed origin (Kierepko et al., 2016; Nalichowska et al., 2023). The ^{238}Pu/$^{239+240}$Pu ratios measured in air filters collected in Vilnius over the years 2005−2006 varied from 0.028 to 0.042, whereas ^{241}Am/$^{239+240}$Pu results fell within the range of 0.19−0.65, both consistent with the GF (+ SNAP 9A) reference. However, ^{238}Pu/$^{239+240}$Pu level as high as 1.2 ± 0.1 was detected in Lithuanian air in March−April of 2011 (Lujaniene et al., 2012). Findings from the surface air in Hornsund during 2007−2021 displayed a similar pattern to ^{238}Pu/$^{239+240}$Pu in Bialystok, Krakow and Vilnius, yet not to ^{241}Am/$^{239+240}$Pu, with the latter being determined solely in Vilnius. Unfortunately, a comparative analysis focused on ^{237}Np could not be performed since no recent reports have detected its presence in the atmosphere.

The provenance of airborne ^{238}Pu enrichment in the European atmosphere remains unclear. The following rationale posited by researchers may also shed more light on Hornsund's situation. Potential sources of plutonium in recently measured aerosol samples have been hypothesised as fuel particles from the Chernobyl or Fukushima accident and emissions from nuclear installations (i.e. nuclear power plants, nuclear research centres or nuclear fuel reprocessing plants) (Wershofen and Arnold, 1998). Hirose and Povinec (Hirose and Povinec, 2015) proposed global desert dust events, biomass burning and the sea spray effect as additional likely delivery mechanisms. Saharan and Asian dust transport has been classified as the most significant event redistributing aerosols in the atmosphere in the mid-latitude region around the globe. The Saharan dust is characterised, however, by isotope ratios typical for global fallout (Chamizo et al., 2010). The Chernobyl ecosystem was affected by several major wildfires, notably in 1992, 1999, 2000, 2002−2004, 2006, 2010, 2015, 2016, 2018 and 2020 (Masson et al., 2021). The dispersion of fly ash particles from biomass fires has been demonstrated to extend over vast distances, both horizontally (up to several thousand kilometres) and vertically (several kilometres), capable of penetrating the tropopause and reaching the lower stratosphere (Hirose and Povinec, 2015). Wildfires in the Chernobyl Exclusion Zone have been confirmed to trigger the dispersion of post-Chernobyl contaminants across Europe in April 2020 (Masson et al., 2021). Furthermore, the contribution of plutonium from sea salt to atmospheric plutonium deposition has been found negligible when compared to soil's (less than 0.3%) (Hirose et al., 2003). The maximum calculated input of sea-spray plutonium to the atmosphere did not exceed 0.006 nBq/m^3, which is by 2–3 orders of magnitude less than that of other plutonium 'feeder' mechanisms.

https://doi.org/10.5194/egusphere-2025-1573
Preprint. Discussion started: 13 May 2025

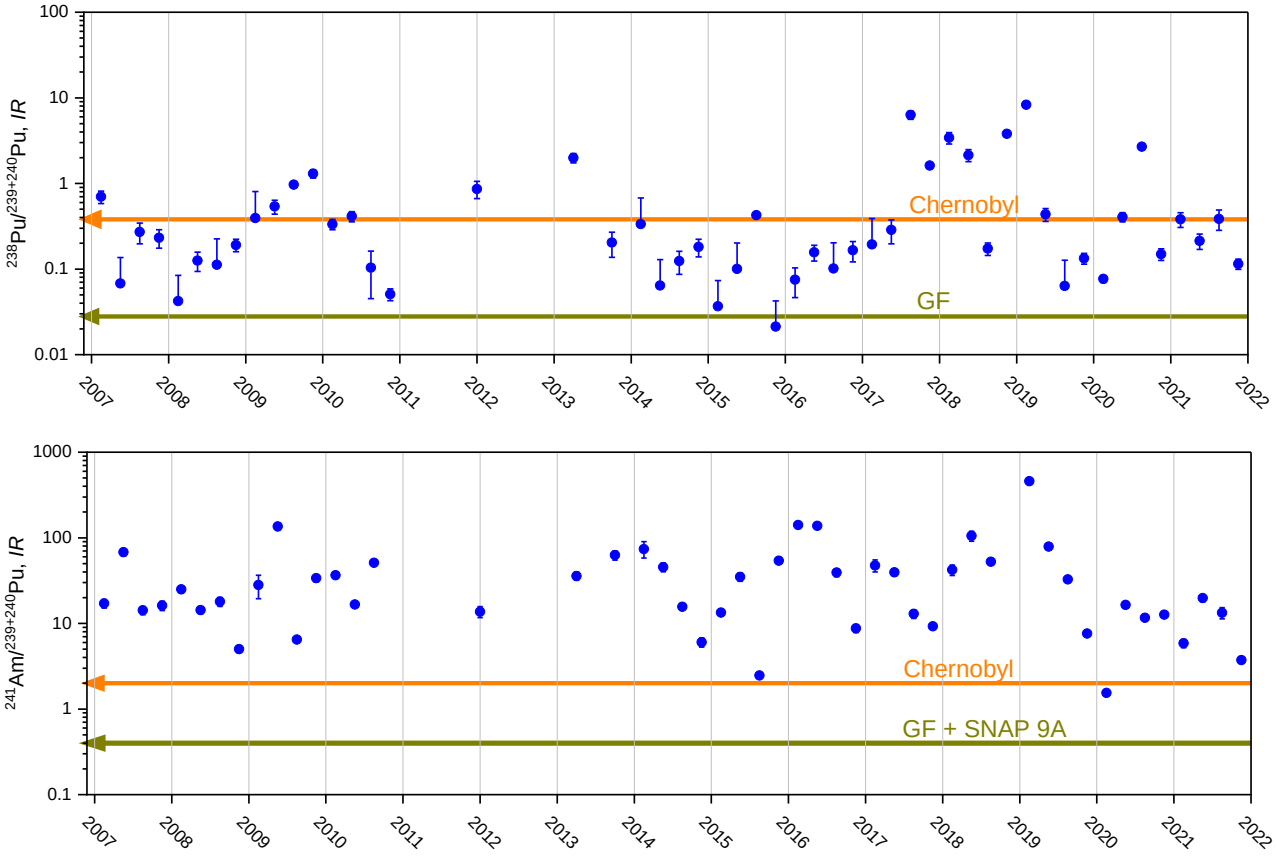

Figure 7: Activity ratios (*IR*) of ^{238}Pu/$^{239+240}$Pu and ^{241}Am/$^{239+240}$Pu for quarterly air filters collected in Hornsund during 2007–2021 (error bars represent 1σ level). GF (+ SNAP 9A) and Chernobyl are used as reference values based on Table S6.

https://doi.org/10.5194/egusphere-2025-1573
Preprint. Discussion started: 13 May 2025

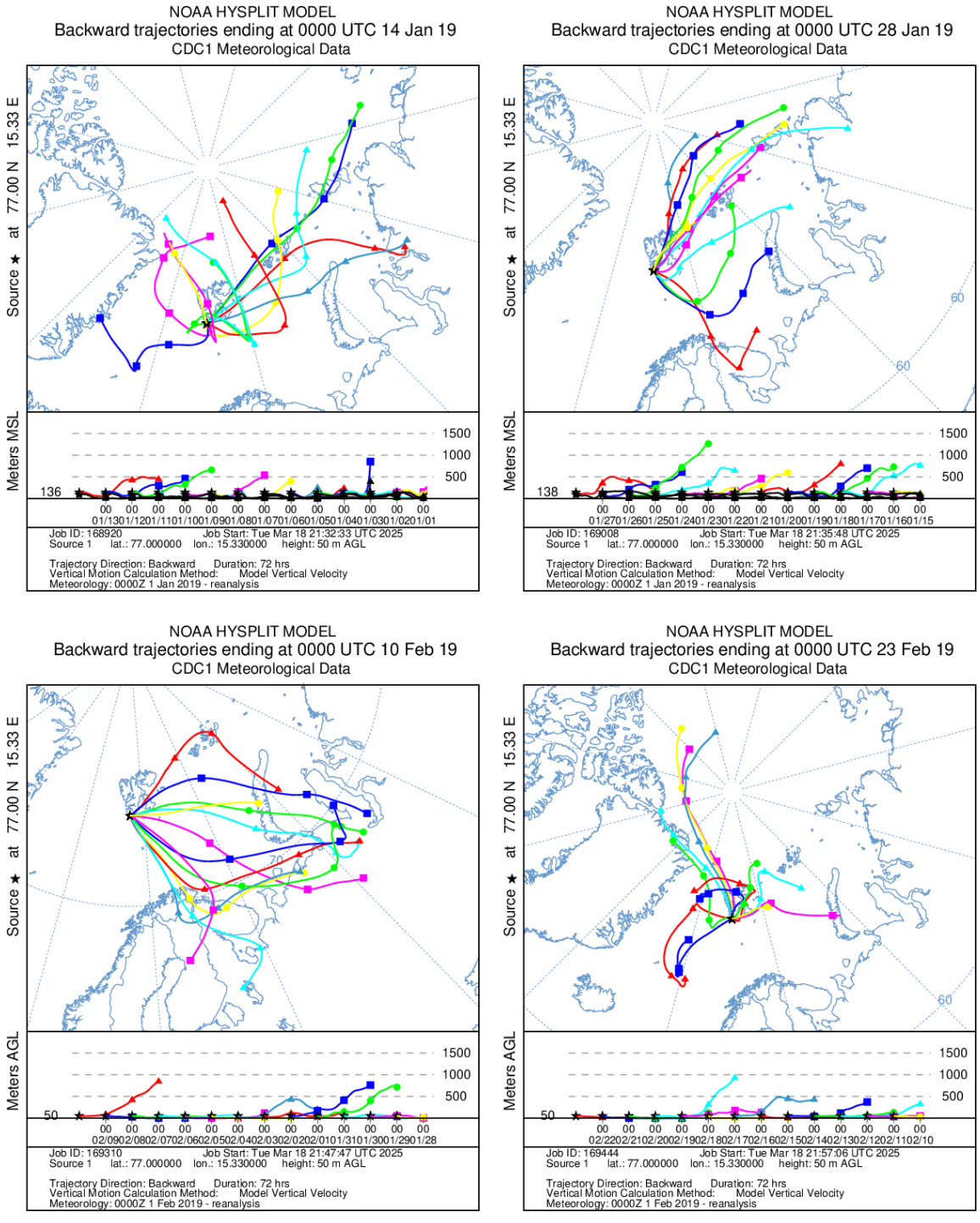

Figure 8: Simulated backward trajectories to a studied area of Hornsund during the 1st quarter of 2019.

https://doi.org/10.5194/egusphere-2025-1573
Preprint. Discussion started: 13 May 2025

The maximum activity concentration of $^{239+240}$Pu in Hornsund coincided with the highest $^{239+240}$Pu level in Krakow, both noted in the 3rd quarter of 2015. This may have indicated a common source behind $^{239+240}$Pu outliers; however, the ^{238}Pu/$^{239+240}$Pu signatures of the aerosol samples were shown to be different. Nalichowska et al. (2023) highlighted the potential supply of air radioactivity from forest fires that occurred on August 8–9, 2015, near the Chernobyl nuclear power plant. Although the ^{238}Pu/$^{239+240}$Pu result in Krakow could not be attributed to the plutonium from spent nuclear fuel, it would explain the situation in Hornsund, as the ^{238}Pu/$^{239+240}$Pu ratio was equal to 0.426 ± 0.017 during the period considered. The elevated $^{239+240}$Pu activity concentration in Krakow was more likely due to intense resuspension processes associated with a high number of local fires in Poland that could remobilise the global fallout plutonium present in forest litter (Nalichowska et al., 2023). Scheduled measurements of ^{240}Pu/^{239}Pu mass ratios should serve to verify whether fly ash particles with different ^{238}Pu/$^{239+240}$Pu signatures were responsible for the 2015 plutonium events in Hornsund and Krakow. However, this line of reasoning fails to explain the remarkable enrichment of ^{241}Am spanning the years 2007−2021, the clear inputs of ^{238}Pu in 2009, 2017, 2018, 2019 and 2020, or the single ^{237}Np incidents in 2013, 2014 and 2018 established for the Hornsund sampling point. Evidence from the correlation and isotopic ratios assessment (Tables 2, 3, 4 and Table S7) suggests that a significant proportion of the ^{238}Pu, ^{237}Np and ^{241}Am must have been introduced into the atmosphere via non-natural emissions. In contrast, $^{239+240}$Pu exhibited a stronger association with environmental processes, such as local resuspension (as reflected by the correlation with *SPM*, Table 3) or long-range transportation with polluted air masses from distant areas (as demonstrated by the correlation with ^{7}Be and ^{210}Pb, Table 4). Perhaps ^{238}Pu was more linked to natural processes than ^{241}Am and ^{237}Np, since the annual changes in ^{238}Pu median values were consistent with those for $^{239+240}$Pu, also expressed by a positive weak correlation of ^{238}Pu vs. $^{239+240}$Pu (Table 4, Fig. 6).

Identification of the exclusive emissions of ^{238}Pu, ^{241}Am and/or ^{237}Np remains challenging in the absence of clear signals of other technogenic radioisotopes. The following examples of past and present nuclear activities have involved single radioisotope applications. ^{238}Pu is characterised by sufficient decay heat to power a deep space satellite or a space probe as a radioisotope thermoelectric generator (RTG). The well-documented source of ^{238}Pu alone is related to the SNAP 9A high atmospheric burn-up in 1964 (Krey, 1967). It is doubtful that ^{238}Pu from the SNAP 9A accident has been present in the stratosphere for the last decades (Hirose and Povinec, 2015). Since the early 2010s, the US government initiated efforts to restart the production of ^{238}Pu heat source material for NASA deep space missions (Urban-Klaehn et al., 2021; Zillmer et al., 2022). The process involves irradiating a ^{237}Np target with neutrons, which converts a portion of ^{237}Np to ^{238}Pu. New production relies on reactors at both Oak Ridge National Laboratory (ORNL) and Idaho National Laboratory (INL). However, recent operations have not been reported to be associated with releases of either ^{238}Pu or ^{237}Np. Radioactive ^{241}Am is commonly used in commercial applications, including precision measuring devices (e.g. industrial flow meters, aviation fuel and thickness gauges) or smoke detectors. The processing of electrical waste, particularly isotopic smoke detectors, has been postulated to account for the ^{241}Am release in 2021 over central Poland (Długosz-Lisiecka and Isajenko, 2024). Smoke detectors have been widespread around the world as a small and very effective means of detecting fires in buildings. The ^{241}Am activity in various models ranged from 7.4 to 740 kBq, distributed under class exemption (NUREG, 2001,

https://doi.org/10.5194/egusphere-2025-1573
Preprint. Discussion started: 13 May 2025

NUREG/CP-0001, 1978, Nuclear Energy Agency, Organisation for Economic Co-operation and Development, OECD, 1977). The estimated total number of smoke detectors currently in use for residential purposes in the USA is approximately 100 million, with a total ^{241}Am activity of 12 TBq. The high cost of the legal storage of spent devices, coupled with no awareness among homeowners, has resulted in a significant number of detectors being disposed of with regular waste or as common e-waste without any control. The recycling of these devices with general waste or their combustion in an incineration plant is becoming more popular every year (Długosz-Lisiecka and Isajenko, 2024). Importantly, ^{241}Am may also be a generator of ^{237}Np, as the latter is a decay product of ^{241}Am.

A series of transport simulations of nuclear aerosols through the troposphere were performed utilising a HYSPLIT model, with a focus exclusively on the 1st quarter of 2019. During this period, the highest activity concentration among the examined artificial actinides was recorded (for ^{241}Am). The dispersion of $^{241}AmO_2$ was investigated based on the total propagation of aerosols over a 72-hour duration and within a range of altitudes up to 1 km. Modelling of trajectories was initiated on January 1st and subsequent tracking was conducted by March 31st, as depicted in Fig. 8 and Fig. S5. The most noteworthy transport pathways from northern Europe and Asia via the island of Novaya Zemlya were noted between January and February (Fig. 8). Nuclear aerosols were carried at low levels in the troposphere (below 100 m), resulting in weak dilution and intense deposition. The obtained trajectories of early February 2019 pointed to significant material shifts from the Novaya Zemlya region to the aerosol sampling point. Simulations in early January, late February and March demonstrated the presence of additional backward wind trajectories derived from northern directions (Fig. S5), that seemed unlikely to transport nuclear aerosols highly enriched in ^{241}Am (or other artificial radioisotopes). Reconstructions of aerosol propagation for the remaining period under study, with lower radioisotope activity concentrations than in the 1st quarter of 2019, were beyond the scope of this paper, but are planned to be continued in upcoming scientific exercises.

Conclusions

The present study focused on the Arctic troposphere, providing an experimental aerosol database that has improved considerably since 1999. The activity concentrations of ^{238}Pu, $^{239+240}$Pu and ^{241}Am in the surface air of Hornsund were determined for the years 2007–2021. While the general levels of ^{238}Pu and $^{239+240}$Pu were comparable to recent observations from different sites, ^{241}Am was found to be extraordinarily high, with a maximum of 354 nBq/m^3 detected in the 1st quarter of 2019. Subsequent analysis of isotopic ratios revealed a frequent enrichment of ^{238}Pu over $^{239+240}$Pu, inconsistent with previously documented releases. Additionally, unexpected single incidents of ^{237}Np were encountered in 2013, 2014 and 2018.

A multivariate analysis incorporating data on ^{7}Be, ^{210}Pb, ^{137}Cs activity concentrations and a wide range of meteorological factors was applied to explain the behaviour of artificial actinides in the lower atmosphere. Evaluation of Spearman correlations allowed explicit links between $^{239+240}$Pu seasonal trends and natural processes, such as local resuspension throughout the year and horizontal tropospheric transport of haze layers from remote areas in the 1st quarter. Similar

https://doi.org/10.5194/egusphere-2025-1573
Preprint. Discussion started: 13 May 2025

mechanisms controlled a certain proportion of ^{238}Pu, but to a lesser extent. The maximum activity concentrations of 6.61 nBq/m^3 for ^{238}Pu and 15.51 nBq/m^3 for $^{239+240}$Pu recorded in Hornsund during the 3rd quarter of 2015, registered simultaneously at middle latitudes, could be related to random events, such as fly ash particles remobilised by wildfires of 2015 occurring, for instance, in proximity to the Chernobyl zone.

A majority of the significantly elevated levels of ^{241}Am, ^{238}Pu and ^{237}Np were found not to be environmentally induced. The average annual doses associated with the exposure to investigated alpha emitters were negligible, being about a million times smaller than the typical background radiation doses of 2.4 mSv per year. Therefore, the contamination detected did not pose a radiological threat to the Arctic environment. Nevertheless, the ^{241}Am, ^{238}Pu and ^{237}Np signals were alarming, as the circumstances of their occurrence could indicate man-made emissions, completely unnoticed by the regular monitoring of gamma emitters in Hornsund air. Trajectory simulations performed for the 1st quarter of 2019 showed the most prominent transport pathways from northern Asia and Europe via the island of Novaya Zemlya. Nuclear aerosols were carried at low levels in the troposphere (below 100 m), resulting in weak dilution and intense deposition. Of note, no radioactive discharges of man-made actinides to air have been declared in the last decades. However, a ^{241}Am incident was identified exclusively in the urban air of central Poland during a few weeks in 2021, possibly generated by the combustion of isotopic smoke detectors. The research highlighted the importance of including alpha emitters in the routine measurements within radiation situation control programmes.

Data availability

Data are available through the Repository of the Institute of Nuclear Physics PAN at https://doi.org/10.48733/no6.25.015.

Author contribution

AC: Writing - original draft, Methodology, Investigation, Formal analysis, Data curation, Conceptualization, Funding acquisition. AB: Methodology, Investigation, Writing - original draft, Methodology, Formal analysis. EN: Writing - original draft, Data curation, Formal analysis, Visualization, Software. MK: Writing - original draft, Resources, Investigation. MD-L: Writing - original draft, Data curation, Formal analysis, Visualization, Writing - original draft. TW: Writing - original draft, Data curation. EŁ: Resources, Writing - original draft. MG: Visualisation. KB: Writing - original draft.

Competing interests

The authors declare that they have no conflict of interest.

Acknowledgements

The authors acknowledge Gabriela Cieślachowska, Katarzyna Barnuś, Mikołaj Wielgat and Michał Palwal for their help during laboratory work.

https://doi.org/10.5194/egusphere-2025-1573
Preprint. Discussion started: 13 May 2025

Financial support

The study was conducted based on the Stanisław Siedlecki Polish Polar Station in Hornsund infrastructure, at the Institute of Geophysics of the Polish Academy of Sciences, financed by the Polish Ministry of Science and Higher Education and contributed to the funding of the Svalbard Integrated Arctic Earth Observing System (SIOS) actions. The National Science Center of Poland supported the research part dedicated to alpha emitter analyses with the project No. 2021/43/D/ST10/02049.

References

Aegerter, S., Bhandari, N., Rama Tamhane, and Tamhane, A. S.: ^{7}Be and ^{32}P in ground level air, Tellus, 18, 212–215, https://doi.org/10.3402/tellusa.v18i2-3.9679, 1966.

Alvarado, J. A. C., Steinmann, P., Estier, S., Bochud, F., Haldimann, M., and Froidevaux, P.: Anthropogenic radionuclides in atmospheric air over Switzerland during the last few decades, Nat Commun, 5, 1–6, https://doi.org/10.1038/ncomms4030, 2014.

AMAP: Radioactivity in the Arctic, Arctic Monitoring and Assessment Programme (AMAP), Oslo, Norway, 2002.

AMAP: Radioactivity in the Arctic, Arctic Monitoring and Assessment Programme (AMAP), Oslo, Norway, 2009.

AMAP: Radioactivity in the Arctic, Arctic Monitoring and Assessment Programme (AMAP), Oslo, Norway, https://doi.org/10.1007/978-1-60327-563-7, 2015.

Baré, J., Gheddou, A., and Kalinowski, M. B.: Overview of temporary radioxenon background measurement campaigns conducted for the CTBTO between 2008 and 2018, J Environ Radioact, 257, https://doi.org/10.1016/j.jenvrad.2022.107053, 2023.

Barrie, L. A., Hoff, R. M., and Daggupaty, S. M.: The influence of mid-latitudinal pollution sources on haze in the Canadian arctic, Atmos Environ, 15, 1407–1419, https://doi.org/10.1016/0004-6981(81)90347-4, 1981.

Beer, J., McCracken, K., and von Steiger, R.: Cosmogenic Radionuclides - Theory and Applications in the Terrestrial and Space Environments, Springer Berlin Heidelberg, 1689–1699 pp., https://doi.org/10.1017/CBO9781107415324.004, 2019.

Błażej, S. and Mietelski, J. W.: Cosmogenic ^{22}Na, ^{7}Be and terrestrial ^{137}Cs, ^{40}K radionuclides in ground level air samples collected weekly in Kraków (Poland) over years 2003-2006, J Radioanal Nucl Chem, 300, 747–756, https://doi.org/10.1007/s10967-014-3049-6, 2014.

Bossew, P., Gering, F., Petermann, E., Hamburger, T., Katzlberger, C., Hernandez-Ceballos, M. A., De Cort, M., Gorzkiewicz, K., Kierepko, R., and Mietelski, J. W.: An episode of Ru-106 in air over Europe, September–October 2017 – Geographical distribution of inhalation dose over Europe, J Environ Radioact, 205–206, 79–92, https://doi.org/10.1016/j.jenvrad.2019.05.004, 2019.

https://doi.org/10.5194/egusphere-2025-1573
Preprint. Discussion started: 13 May 2025

Burakowska, A., Kubicki, M., Mysłek-Laurikainen, B., Piotrowski, M., Trzaskowska, H., and Sosnowiec, R.: Concentration of ^{7}Be, ^{210}Pb, ^{40}K, ^{137}Cs, ^{134}Cs radionuclides in the ground layer of the atmosphere in the polar (Hornsund, Spitsbergen) and mid-latitudes (Otwock-Świder, Poland) regions, J Environ Radioact, 240, https://doi.org/10.1016/j.jenvrad.2021.106739, 2021.

Chamizo, E., García-León, M., Enamorado, S. M., Jiménez-Ramos, M. C., and Wacker, L.: Measurement of plutonium isotopes, ^{239}Pu and ^{240}Pu, in air-filter samples from Seville (2001-2002), Atmos Environ, 44, 1851–1858, https://doi.org/10.1016/j.atmosenv.2010.02.030, 2010.

Coyne, J., Bobrov, D., Bormann, P., Duran, E., Grenard, P., Haralabus, G., Kitov, I., and Starovoit, Y.: CTBTO: Goals, networks, data analysis and data availability, in: New manual of seismological observatory practice 2 (NMSOP-2), Deutsches GeoForschungsZentrum GFZ, 1–41, https://doi.org/10.2312/GFZ.NMSOP-2, 2012.

Currie, L. A.: Limits for Qualitative Detection and Quantitative Determination: Application to Radiochemistry, Anal Chem, 40, 586–593, https://doi.org/10.1021/ac60259a007, 1968.

Długosz-Lisiecka, M. and Isajenko, K.: Am-241 in the urban air – Monitoring and simulation results, Process Safety and Environmental Protection, 186, 639–644, https://doi.org/10.1016/j.psep.2024.03.124, 2024.

Dueñas, C., Fernández, M. C., Carretero, J., Liger, E., and Cañete, S.: Atmospheric deposition of ^{7}Be at a coastal Mediterranean station, Journal of Geophysical Research Atmospheres, 106, 34059–34065, https://doi.org/10.1029/2001JD000771, 2001.

Engelbrecht, R. and Schwaiger, M.: State of the art of standard methods used for environmental radioactivity monitoring, Applied Radiation and Isotopes, 66, 1604–1610, https://doi.org/10.1016/j.apradiso.2008.01.021, 2008.

Eriksson, M., Holm, E., Roos, P., and Dahlgaard, H.: Distribution and flux of ^{238}Pu, ^{239,240}Pu, ^{241}Am, ^{137}Cs and ^{210}Pb to high arctic lakes in the Thule district (Greenland), J Environ Radioact, 75, 285–299, https://doi.org/10.1016/j.jenvrad.2003.12.007, 2004.

Feely, H. W., Helfer, I. K., Juzdan, Z. R., Klusek, C. S., Larsen, R. J., Leifer, R., Sanderson, C. G., and Dreicer, M.: Fallout in the New York metropolitan area following the chernobyl accident, J Environ Radioact, 7, 177–191, https://doi.org/10.1016/0265-931X(88)90006-9, 1988.

Feely, H. W., Larsen, R. J., and Sanderson, C. G.: Factors that cause seasonal variations in Beryllium-7 concentrations in surface air, J Environ Radioact, 9, 223–249, https://doi.org/10.1016/0265-931X(89)90046-5, 1989.

Furuno, A., Ohmori, R., Tateoka, H., Minakawa, Y., Kurihara, T., Yamamoto, Y., and Tomita, Y.: Assessment of Caesium-137 Detections at CTBTO Radionuclide Monitoring Stations in East Asia and Their Relationship to Asian Dust Dispersion, Pure Appl Geophys, https://doi.org/10.1007/s00024-024-03620-y, 2024.

Gäggeler, H. W.: Radioactivity in the Atmosphere, Ract, 70–71, 345–354, https://doi.org/10.1524/ract.1995.7071.special-issue.345, 1995.

https://doi.org/10.5194/egusphere-2025-1573
Preprint. Discussion started: 13 May 2025

Gorzkiewicz, K., Kierepko, R., Paatero, J., Virkkula, A., and Mietelski, J. W.: Air radioactivity in Marambio Base: The peculiar character of Antarctic Peninsula, J Environ Radioact, 251–252, 106930, https://doi.org/10.1016/j.jenvrad.2022.106930, 2022.

Grossi, C., Ballester, J., Serrano, I., Galmarini, S., Camacho, A., Curcoll, R., Morguí, J. A., Rodò, X., and Duch, M. A.: Influence of long-range atmospheric transport pathways and climate teleconnection patterns on the variability of surface ^{210}Pb and ^{7}Be concentrations in southwestern Europe, J Environ Radioact, 165, 103–114, https://doi.org/10.1016/j.jenvrad.2016.09.011, 2016.

Gwynn, J. P., Dowdall, M., Davids, C., Selnæs, Ø. G., and Lind, B.: The radiological environment of Svalbard, Polar Res, 23, 167–180, https://doi.org/10.1111/j.1751-8369.2004.tb00006.x, 2004.

Hirose, K. and Povinec, P. P.: Sources of plutonium in the atmosphere and stratosphere-troposphere mixing, Sci Rep, 5, 1–9, https://doi.org/10.1038/srep15707, 2015.

Hirose, K., Igarashi, Y., Aoyama, M., Kim, C. K., Kim, C. S., and Chang, B. W.: Recent trends of plutonium fallout observed in Japan: Plutonium as a proxy for desertification, Journal of Environmental Monitoring, 5, 302–307, https://doi.org/10.1039/b212560a, 2003.

Hoover, M. D. and Maiello, M. L.: Radioactive Air Sampling Methods, CRC Press Taylor & Francis Group, Boca Raton London New York, 1–581 pp., https://doi.org/10.1097/hp.0b013e318217066b, 2010.

ICRP: 1990 Recommendations of the International Commission on Radiological Protection. ICRP Publication 60, Ann ICRP, 21, 1991.

ICRP: The 2007 Recommendations of the International Commission on Radiological Protection. ICRP Publication 103, Ann ICRP, 37, 2007.

IPCC: IPCC Special Report on the Ocean and Cryosphere in a Changing Climate, edited by: Pörtner, H.-O., Roberts, D. C., Masson-Delmotte, V., Zhai, P., Tignor, M., Poloczanska, E., Mintenbeck, K., Alegría, A., Nicolai, M., Okem, A., Petzold, J., Rama, B., and Weyer, N. M., Cambridge University Press, Cambridge, UK and New York, NY, USA, https://doi.org/10.1017/CBO9781139177245.003, 2019.

Kelley, J. M., Bond, L. A., and Beasley, T. M.: Global distribution of Pu isotopes and ^{237}Np, Science of the Total Environment, 237–238, 483–500, https://doi.org/10.1016/S0048-9697(99)00160-6, 1999.

Kierepko, R., Mietelski, J. W., Ustrnul, Z., Anczkiewicz, R., Wershofen, H., Holgye, Z., Kapała, J., and Isajenko, K.: Plutonium isotopes in the atmosphere of Central Europe: Isotopic composition and time evolution vs. circulation factors, Science of the Total Environment, 569–570, 937–947, https://doi.org/10.1016/j.scitotenv.2016.05.222, 2016.

Koo, Y. H., Yang, Y. S., and Song, K. W.: Radioactivity release from the Fukushima accident and its consequences: A review, Progress in Nuclear Energy, 74, 61–70, https://doi.org/10.1016/j.pnucene.2014.02.013, 2014.

Krey, P. W.: Atmospheric burnup of a plutonium-238 generator, Science (1979), 158, 769–771, https://doi.org/10.1126/science.158.3802.769, 1967.

https://doi.org/10.5194/egusphere-2025-1573
Preprint. Discussion started: 13 May 2025

Kulan, A., Aldahan, A., Possnert, G., and Vintersved, I.: Distribution of ^{7}Be in surface air of Europe, Atmos Environ, 40, 3855–3868, https://doi.org/10.1016/j.atmosenv.2006.02.030, 2006.

Larsen, R. J.: Letter To The Editor: Global Decrease of Beryllium in Surface Air, J Environ Radioact, 18, 85–87, https://doi.org/10.1080/13518040701205365, 1993.

Larsen, R. J.: Letter To The Editor: Fission Products Detected in Alaska Following the Tomsk-7 Accident, Int J Phytoremediation, 23, 205–209, https://doi.org/10.1080/13518040701205365, 1994.

Larsen, R. J., Haagenson, P. L., and Reiss, N. M.: Transport processes associated with the initial elevated concentrations of Chernobyl radioactivity in surface air in the United States, J Environ Radioact, 10, 1–18, https://doi.org/10.1016/0265-931X(89)90002-7, 1989.

Larsen, R. J., Sanderson, C. G., and Kada, J.: EML Surface Air Sampling Program, 1990-1993 Data, New York, 1995.

Lee, H. N. and Feichter, J.: An intercomparison of wet precipitation scavenging schemes and the emission rates of ^{222}Rn for the simulation of global transport and deposition of ^{210}Pb, J Geophys Res, 100, https://doi.org/10.1029/95jd01732, 1995.

Łokas, E., Mietelski, J. W., Ketterer, M. E., Kleszcz, K., Wachniew, P., Michalska, S., and Miecznik, M.: Sources and vertical distribution of ^{137}Cs, ^{238}Pu, $^{239+240}$Pu and ^{241}Am in peat profiles from southwest Spitsbergen, Applied Geochemistry, 28, 100–108, https://doi.org/10.1016/j.apgeochem.2012.10.027, 2013.

Łokas, E., Zaborska, A., Kolicka, M., Różycki, M., and Zawierucha, K.: Accumulation of atmospheric radionuclides and heavy metals in cryoconite holes on an Arctic glacier, Chemosphere, 160, 162–172, https://doi.org/10.1016/j.chemosphere.2016.06.051, 2016.

Łokas, E., Wachniew, P., Jodłowski, P., and Gąsiorek, M.: Airborne radionuclides in the proglacial environment as indicators of sources and transfers of soil material, J Environ Radioact, 178–179, 193–202, https://doi.org/10.1016/j.jenvrad.2017.08.018, 2017a.

Łokas, E., Zwoliński, Z., Rachlewicz, G., Gąsiorek, M., Wilkosz, G., and Samolej, K.: Distribution of anthropogenic and naturally occurring radionuclides in soils and lakes of Central Spitsbergen (Arctic), J Radioanal Nucl Chem, 311, 707–717, https://doi.org/10.1007/s10967-016-5085-x, 2017b.

Lujaniene, G., Valiulis, D., Byčenkien, S., Šakalys, J., and Povinec, P. P.: Plutonium isotopes and ^{241}Am in the atmosphere of Lithuania: A comparison of different source terms, Atmos Environ, 61, 419–427, https://doi.org/10.1016/j.atmosenv.2012.07.046, 2012.

Marsz, A. and Styszyńska, A.: Climate and Climate Change at Hornsund, Svalbard, Gdynia Maritime University, Gdynia, 2013.

Masson, O., Piga, D., Gurriaran, R., and D'Amico, D.: Impact of an exceptional Saharan dust outbreak in France: PM10 and artificial radionuclides concentrations in air and in dust deposit, Atmos Environ, 44, 2478–2486, https://doi.org/10.1016/j.atmosenv.2010.03.004, 2010.

Masson, O., Romanenko, O., Saunier, O., Kirieiev, S., Protsak, V., Laptev, G., Voitsekhovych, O., Durand, V., Coppin, F., Steinhauser, G., De Vismes Ott, A., Renaud, P., Didier, D., Boulet, B., Morin, M., Hýža, M., Camps, J., Belyaeva, O.,

https://doi.org/10.5194/egusphere-2025-1573
Preprint. Discussion started: 13 May 2025

Dalheimer, A., Eleftheriadis, K., Gascó-Leonarte, C., Ioannidou, A., Isajenko, K., Karhunen, T., Kastlander, J., Katzlberger, C., Kierepko, R., Knetsch, G. J., Kónyi, J. K., Mietelski, J. W., Mirsch, M., Møller, B., Nikolić, J. K., Rusconi, R., Samsonov, V., Simion, E., Steinmann, P., Stoulos, S., Suarez-Navarro, J. A., Wershofen, H., Zapata-García, D., and Zorko, B.: Europe-Wide Atmospheric Radionuclide Dispersion by Unprecedented Wildfires in the Chernobyl Exclusion Zone, April 2020, Environ Sci Technol, 55, 13834–13848, https://doi.org/10.1021/acs.est.1c03314, 2021.

Mietelski, J. W. and Povinec, P. P.: Environmental radioactivity aspects of recent nuclear accidents associated with undeclared nuclear activities and suggestion for new monitoring strategies, J Environ Radioact, 214–215, 106151, https://doi.org/10.1016/j.jenvrad.2019.106151, 2020.

Mietelski, J. W., Gaca, P., and Olech, M. A.: Radioactive contamination of lichens and mosses collected in South Shetlands and Antarctic Peninsula, 245, 527–537, 2000.

Mietelski, J. W., Kubica, B., Gaca, P., Tomankiewicz, E., Błażej, S., Tuteja-Krysa, M., and Stobiński, M.: ^{238}Pu, $^{239+240}$Pu, ^{241}Am, ^{90}Sr and ^{137}Cs in mountain soil samples from the Tatra National Park (Poland), J Radioanal Nucl Chem, 275, 523–533, https://doi.org/10.1007/s10967-007-7026-1, 2008.

Mukaka, M. M.: Correlation coefficient and its use, Malawi Medical Journal, 24, 69–71, 2012.

Nalichowska, E., Mietelski, J. W., Kierepko, R., Ustrnul, Z., Gorzkiewicz, K., Brudecki, K., and Kowalska, A.: Plutonium isotopes in the ground air layer in southern Poland (2010–2016): Source terms, seasonal variability and correlations with meteorological conditions, J Environ Radioact, 264, 107204, https://doi.org/10.1016/j.jenvrad.2023.107204, 2023.

Oughton, D., Day, P., and Fifield, K.: Plutonium measurement using accelerator mass spectrometry: Methodology and applications, Radioactivity in the Environment, 1, 47–62, https://doi.org/10.1016/S1569-4860(01)80006-1, 2001.

Paatero, J., Hatakka, J., Holmén, K., Eneroth, K., and Viisanen, Y.: Lead-210 concentration in the air at Mt. Zeppelin, Ny-Ålesund, Svalbard, Physics and Chemistry of the Earth, 28, 1175–1180, https://doi.org/10.1016/j.pce.2003.08.050, 2003.

Paatero, J., Buyukay, M., Holmén, K., Hatakka, J., and Viisanen, Y.: Seasonal variation and source areas of airborne lead-210 at Ny-Ålesund in the High Arctic, Polar Res, 29, 345–352, https://doi.org/10.1111/j.1751-8369.2010.00185.x, 2010.

Povinec, P. P., Gera, M., Holý, K., Hirose, K., Lujanienė, G., Nakano, M., Plastino, W., Sýkora, I., Bartok, J., and Gažák, M.: Dispersion of Fukushima radionuclides in the global atmosphere and the ocean, Applied Radiation and Isotopes, 81, 383–392, https://doi.org/10.1016/j.apradiso.2013.03.058, 2013.

Qiao, J., Hou, X., Roos, P., and Miró, M.: Rapid and simultaneous determination of neptunium and plutonium isotopes in environmental samples by extraction chromatography using sequential injection analysis and ICP-MS, J Anal At Spectrom, 25, 1769–1779, https://doi.org/10.1039/c003222k, 2010.

Qiao, J., Hou, X., Steier, P., and Golser, R.: Sequential injection method for rapid and simultaneous determination of ^{236}U, ^{237}Np, and Pu isotopes in seawater, Anal Chem, 85, 11026–11033, https://doi.org/10.1021/ac402673p, 2013.

Rahn, K. A.: Relative importances of North America and Eurasia as sources of arctic aerosol, Atmospheric Environment (1967), 15, 1447–1455, https://doi.org/10.1016/0004-6981(81)90351-6, 1981.

https://doi.org/10.5194/egusphere-2025-1573
Preprint. Discussion started: 13 May 2025

Rinke, A., Maturilli, M., Graham, R. M., Matthes, H., Handorf, D., Cohen, L., Hudson, S. R., and Moore, J. C.: Extreme cyclone events in the Arctic: Wintertime variability and trends, Environmental Research Letters, 12, https://doi.org/10.1088/1748-9326/aa7def, 2017.

La Rosa, J. J., Cooper, E. L., Ghods-Esphahani, A., Jansta, V., Makarewicz, M., Shawky, S., and Vajda, N.: Radiochemical methods used by the IAEA's laboratories at Seibersdorf for the determination of ^{90}Sr, ^{144}Ce and Pu radionuclides in environmental samples collected for the International Chernobyl project, J Environ Radioact, 17, 183–209, https://doi.org/10.1016/0265-931X(92)90025-O, 1992.

La Rosa, J., Gastaud, J., Lagan, L., Lee, S. H., Levy-Palomo, I., Povinec, P. P., and Wyse, E.: Recent developments in the analysis of transuranics (Np, Pu, Am) in seawater, J Radioanal Nucl Chem, 263, 427–436, https://doi.org/10.1007/s10967-005-0072-7, 2005.

Schober, P. and Schwarte, L. A.: Correlation coefficients: Appropriate use and interpretation, Anesth Analg, 126, 1763–1768, https://doi.org/10.1213/ANE.0000000000002864, 2018.

Stein, A. F., Draxler, R. R., Rolph, G. D., Stunder, B. J. B., Cohen, M. D., and Ngan, F.: Noaa's hysplit atmospheric transport and dispersion modeling system, Bull Am Meteorol Soc, 96, 2059–2077, https://doi.org/10.1175/BAMS-D-14-00110.1, 2015.

Steinhauser, G., Brandl, A., and Johnson, T. E.: Comparison of the Chernobyl and Fukushima nuclear accidents: A review of the environmental impacts, Science of the Total Environment, 470–471, 800–817, https://doi.org/10.1016/j.scitotenv.2013.10.029, 2014.

UNSCEAR: Annex E: Exposures resulting from nuclear explosions. Report of the Nations Scientific Committee on the Effects of Atomic Radiation., in: United Nations Scientific Committee on the Effects of Atomic Radiation, https://doi.org/10.1080/09553008314550691, 1982.

UNSCEAR: Annex A: Exposures from natural sources of radiation, UNSCEAR 1993 Report to the general assembly, with scientific annexes, 1993.

UNSCEAR: Annex C: Exposures to the Public from Man-Made Sources of Radiation. Report of the United Nations Scientific Committee on the Effects of Atomic Radiation., 2000a.

UNSCEAR: Annexes J: Exposure and Effects of Chernobyl Accident, 2000b.

Urban-Klaehn, J., Miller, D., Gross, B. J., Tyler, C. R., and Dwight, C. C.: Initial phase of Pu-238 production in Idaho National Laboratory, Applied Radiation and Isotopes, 169, https://doi.org/10.1016/j.apradiso.2020.109517, 2021.

Wawrzyniak, T. and Osuch, M.: A 40-year High Arctic climatological dataset of the Polish Polar Station Hornsund (SW Spitsbergen, Svalbard), Earth Syst Sci Data, 12, 805–815, https://doi.org/10.5194/essd-12-805-2020, 2020.

Wershofen, H. and Arnold, D.: Radionuclides in Ground-level Air in Braunschweig-Report of the PTB Trace Survey Station Physikalisch-Technische Bundesanstalt, 1998.

https://doi.org/10.5194/egusphere-2025-1573
Preprint. Discussion started: 13 May 2025

Zhang, W., Paatero, J., Leppänen, A. P., Møller, B., Jensen, L. K., Gudnason, K., Sofiev, M., Anderson, P., Sickel, M., Burakowska, A., Kubicki, M., and Anderson, A.: Evaluation of 137Cs, 133Xe and 3H activity concentrations monitored in the Arctic atmosphere, J Environ Radioact, 253–254, https://doi.org/10.1016/j.jenvrad.2022.107013, 2022.

875 Zillmer, A., Green, W., Tyler, C., Gross, B., Rosvall, E., Fradeneck, A., Fishler, J., Reeder, D., Marlow, R., Urban-Klaehn, J., Reichenberger, M., Hill, M., and Howard, R.: Recent 238Pu Production Activities at Idaho National Laboratory, Nucl Technol, 208, S1–S10, https://doi.org/10.1080/00295450.2022.2105774, 2022.